1	Photo sensing and quorum sensing are integrated to control Pseudomonas aeruginosa
2	collective behaviors.
3	
4	Sampriti Mukherjee ¹ , Matthew Jemielita ¹ , Vasiliki Stergioula ¹ , Mikhail Tikhonov ² and Bonnie L.
5	Bassler*1,3
6	
7	¹ Princeton University, Department of Molecular Biology, Princeton, NJ 08544, USA.
8	² Physics department, Washington University in St Louis, St Louis, MO 63130, USA.
9	³ Howard Hughes Medical Institute, Chevy Chase, MD 20815, USA.
10	*Correspondence to: <u>bbassler@princeton.edu</u>
11	
12	
13	
14	
15	Short title: Photo sensing and quorum sensing converge to control bacterial group behaviors.
16	
17	
18	
19	
20	
21	
22	
23	

ABSTRACT

24

25

26

27

28

29

30

31

32

33

34

35

36

37

38

39

40

41

42

Bacteria convert changes in sensory inputs into alterations in gene expression, behavior, and lifestyles. A common lifestyle choice bacteria make is whether to exhibit individual behavior and exist in the free-living planktonic state or to engage in collective behavior and form sessile communities called biofilms. Transitions between individual and collective behaviors are controlled by the chemical cell-to-cell communication process called quorum sensing. Here, we show that quorum sensing represses P. aeruginosa biofilm formation and virulence by activating expression of genes encoding the KinB-AlgB two-component system. Phospho-AlgB represses biofilm and virulence genes, while KinB dephosphorylates, and thereby, inactivates AlgB. We discover that the photoreceptor BphP is the kinase that, in response to light, phosphorylates and activates AlgB. Indeed, exposing P. aeruginosa to light represses biofilm formation and virulence gene expression. To our knowledge, P. aeruginosa was not previously known to detect and respond to light. The KinB-AlgB-BphP module is present in all Pseudomonads, and we demonstrate that AlgB is the cognate response regulator for BphP in diverse bacterial phyla. We propose that KinB-AlgB-BphP constitutes a "three-component" system with AlgB acting as the node at which varied sensory information is integrated. This network architecture provides a mechanism enabling the bacteria to integrate at least two different sensory inputs, quorum sensing and light, into the control of collective behaviors. This study sets the stage for lightmediated control of *P. aeruginosa* infectivity.

43

44

45

46

47

Keywords: bacteria, *Pseudomonas*, quorum sensing, photo sensing, biofilms, virulence, two-component system

INTRODUCTION

48

49

50

51

52

53

54

55

56

57

58

59

60

61

62

63

64

65

66

67

68

69

70

71

72

Bacterial responses to self-generated and exogenous stimuli influence their survival, persistence in particular niches, and lifestyle transitions, such as alterations between being freeswimming or existing as a member of a biofilm. Biofilms are three-dimensional structured communities of bacterial cells encased in an extracellular matrix [1,2]. Bacteria living in biofilms exhibit superior resilience to environmental stresses such as antimicrobials and host immune responses [2,3]. Frequently, biofilm formation is governed by intracellular signaling molecules such as cyclic di-GMP [4,5] and extracellular signaling molecules such as quorum-sensing autoinducers [6,7]. Quorum sensing is a cell-to-cell communication process that relies on the production, release, and population-wide detection of autoinducers [8,9]. Quorum sensing allows groups of bacteria to synchronously alter behavior in response to changes in the population density and species composition of the vicinal community. Many pathogenic bacteria, including the global pathogen Pseudomonas aeruginosa, require quorum sensing to establish successful infections [10]. Here, we show that quorum-sensing signaling converges with the detection of and response to another sensory cue, light, to control biofilm formation and virulence factor production in P. aeruginosa. We define the pathway connecting the light and quorum sensing inputs to the virulence and biofilm outputs.

Light is a common environmental cue that is detected by photoreceptors present in all domains of life [11,12]. Particular photoreceptor photosensory domains are activated by specific wavelengths of light [13]. Photoreceptors fall into six families depending on the structure of the light-absorbing chromophore: rhodopsins, xanthopsins, cryptochromes, LOV domain-containing phototropins, blue-light sensing using flavin (BLUF)-domain proteins, and phytochromes [12,13]. In bacteria, the most abundant photoreceptors are phytochromes [14], typically possessing an amino-terminal chromophore-binding domain and a carboxy-terminal histidine kinase (HK) domain. Bacteriophytochromes assemble with the chromophore called biliverdin [15].

Surprisingly, very few bacteria encode a cognate response regulator (RR) in close proximity to the gene specifying the bacteriophytochrome [16], leaving the systems mostly undefined.

73

74

75

76

77

78

79

80

81

82

83

84

85

86

87

88

89

90

91

92

93

94

95

96

97

98

In the human pathogen P. aeruginosa, LuxR-type quorum-sensing receptors, that function as transcriptional activators when they are bound to their cognate autoinducers, are required for virulence and biofilm formation [17,18]. In this study, we examine the mechanism by which the P. aeruginosa LuxR-type quorum-sensing receptor called RhIR represses biofilm formation. A genetic screen reveals that RhIR activates the expression of the algB-kinB operon encoding a two-component system (TCS) in which KinB and AlgB are the sensor HK and cognate RR, respectively [19] (Fig 1). We find that AlgB~P is a repressor of biofilm formation and virulence gene expression. KinB is a phosphatase that dephosphorylates, and thereby inactivates AlgB. Using genetic suppressor analysis and in vitro phosphorylation assays, we discover that BphP is the HK that phosphorylates and activates AlgB, enabling AlgB to repress biofilm formation and genes encoding virulence factors (Fig 1). BphP is a far-red light sensing bacteriophytochrome [20], and indeed, we demonstrate that P. aeruginosa biofilm formation and virulence gene expression are repressed by far-red light. Phylogenetic analyses show that the KinB-AlgB-BphP module is conserved in all Pseudomonads and, moreover, AlgB is present in the majority of bacteria that possess BphP orthologs. This final finding suggests that the BphP-AlgB interaction is widespread. As proof of this notion, we show that P. aeruginosa BphP can phosphorylate AlgB orthologs from α -, β -, and γ -Proteobacteria. Thus, KinB-AlgB-BphP constitute a "three-component" system, and we propose that AlgB functions as the integrator that conveys multiple environmental cues including those specifying population density and the presence or absence of light into the regulation of collective behaviors (Fig 1). We further predict that AlgB functions as the cognate RR for BphP in all bacteria that possess BphP as an orphan HK. The downstream signal transduction components and the outputs of photo sensory cascades are not known in the majority of non-photosynthetic bacteria that possess them making their physiological roles difficult to discern. This study provides the entire cascade—light as the input, BphP as the detector, AlgB as the signal transducer, and biofilm formation and virulence factor production as the outputs—enabling insight into light-driven control of bacterial behaviors.

102

103

104

105

106

107

108

109

110

111

112

113

114

115

116

117

118

119

120

121

122

123

99

100

101

RESULTS

KinB activates and AlgB represses RhIR-dependent group behaviors. We recently discovered that the P. aeruginosa quorum-sensing receptor RhIR represses biofilm formation [21,22]. Specifically, on Congo red agar biofilm medium, wildtype (WT) P. aeruginosa UCBPP-PA14 (hereafter called PA14) exhibits a rugose-center/smooth-periphery colony biofilm phenotype, while the \(\Delta rhIR \) mutant forms a larger hyper-rugose biofilm (Fig 2A). To determine the mechanism by which RhIR impedes biofilm formation, we randomly mutagenized the $\Delta rhIR$ strain using the Tn5 IS50L derivative IS/acZ/hah [23] and screened for colonies exhibiting either a WT or a smooth colony biofilm phenotype. Our rationale was that inactivation of a gene(s) encoding a component that functions downstream of RhIR in biofilm formation would sever the connection between RhIR and repression of biofilm formation. We screened 5,000 transposon insertion mutants. Strains harboring insertions located in genes encoding hypothetical proteins, proteins involved in twitching motility, and proteins required for Pel polysaccharide synthesis all produced smooth colony biofilms (Table S1). Most of these genes were already known to play roles in P. aeruginosa biofilm formation (Fazli et al., 2014). Here, we focus on one transposon insertion mutant that exhibited a smooth colony biofilm phenotype that mapped to the gene PA14 72390 encoding the KinB transmembrane HK (Fig 2A) [19,24,25]. kinB is located immediately downstream of algB in a di-cistron that is conserved in all sequenced Pseudomonads (Fig S1A). To verify that KinB plays a role in biofilm formation, we generated an in-frame marker-less deletion of kinB in the chromosomes of the WT and the $\Delta rhlR$ strains. Both the $\Delta kinB$ single and $\Delta rhlR$ $\Delta kinB$ double mutants failed to form biofilms and instead exhibited

smooth colony phenotypes (Fig 2A). Introduction of a plasmid carrying the kinB gene conferred a hyper-rugose phenotype to the WT and restored biofilm formation to the $\Delta kinB$ and $\Delta rhlR$ $\Delta kinB$ mutants (Fig 2A). By contrast, introduction of a plasmid carrying rhlR did not alter the smooth biofilm phenotype of the $\Delta rhlR$ $\Delta kinB$ mutant (Fig 2A). We conclude that, in P. aeruginosa, KinB is essential for biofilm formation, KinB is an activator of biofilm formation, and KinB functions downstream of RhlR in the biofilm formation process.

PA14 requires Pel, the primary biofilm matrix exopolysaccharide for biofilm formation [26] (Note: PA14 does not produce the Psl exopolysaccharide and alginate does not contribute significantly to the PA14 biofilm matrix, unlike in *P. aeruginosa* PAO1 [27]). To examine if the mechanism by which KinB alters biofilm formation is by changing Pel production, we performed quantitative RT-PCR analyses on WT and $\Delta kinB$ biofilms probing for the expression of the housekeeping gene rpoD as a control and the Pel biosynthetic gene pelA (Fig 2B). Expression of rpoD did not change between the WT and the $\Delta kinB$ mutant, while transcription of pelA was ~14-fold lower in the $\Delta kinB$ strain than in the WT. We conclude that KinB activates Pel production, which is why KinB is required for PA14 biofilm formation.

KinB is a transmembrane HK that undergoes autophosphorylation and then transfers the phosphate to its cognate RR AlgB [19]. To determine if AlgB functions downstream of KinB to control biofilm formation, we introduced a stop codon in place of the codon specifying residue 10 in the algB gene to obtain an $algB^{STOP}$ mutant. The $algB^{STOP}$ mutant had a biofilm phenotype indistinguishable from the WT (Fig 2A). However, introduction of the $algB^{STOP}$ mutation into the $\Delta kinB$ strain restored biofilm formation (Fig 2A). Furthermore, overexpression of algB repressed biofilm formation in the WT as evidenced by the resulting smooth colony biofilm phenotype (Fig 2A). Overexpression of algB also repressed biofilm formation in the $algB^{STOP}$ and algB strains (Fig 2A). Thus, KinB activates while AlgB represses biofilm development.

AlgB has an amino-terminal domain containing the site of phosphorylation (residue D59), a central ATP-binding domain, and a carboxy-terminal helix-turn-helix motif for binding DNA (Fig S1B, S2) [19,28]. AlgB is a member of the NtrC subfamily of RRs and it possesses the hallmark GAFTGA motif required for interaction with RpoN (σ^{54}) [29]. Typically, NtrC-type RRs act as transcriptional activators when they are phosphorylated [30]. To investigate if phosphorylation of AlgB is required for repression of biofilm formation, we substituted the aspartate at residue 59 with an asparagine residue to preclude phosphorylation [28]. We overexpressed the $algB^{D59N}$ allele in the PA14 strain carrying the $algB^{STOP}$ mutation. Unlike WT AlgB, AlgB^{D59N} failed to repress biofilm formation (Fig 2A). To ensure the validity of this result, we generated aminoterminal 3xFLAG tagged algB and $algB^{D59N}$ fusions and expressed them from a plasmid in the $algB^{STOP}$ mutant. Western blot showed that both proteins are produced at similar levels (Fig S3A). We conclude that the phosphorylated form of AlgB is active and is required for AlgB-mediated repression of biofilm development. We presume that AlgB~P functions indirectly as a transcriptional activator to promote the expression of a gene(s) encoding a negative regulator of biofilm formation (Fig 1).

Our results show that AlgB functions downstream of KinB and that KinB and AlgB have opposing activities with respect to PA14 biofilm formation. *In vitro*, KinB possess both kinase and phosphatase activities [25]. One mechanism by which KinB could antagonize AlgB function is by acting as a phosphatase that dephosphorylates AlgB, rendering it inactive. To test this possibility, we integrated the 3xFLAG tagged algB allele at the native algB locus in the chromosomes of WT PA14 and the $\Delta kinB$ mutant. Biofilm analyses show that 3xFLAG-AlgB is functional (Fig S3B). Next, we assessed the phosphorylation status of 3xFLAG-AlgB in vivo. Fig 2C shows that AlgB~P accumulates in the $\Delta kinB$ mutant compared to in the WT. To verify these claims regarding the signal transduction mechanism, we engineered a missense mutation into KinB at a conserved proline (P390) that is required for phosphatase activity [25]. Specifically, we

generated both kinB-SNAP and $kinB^{P390S}$ -SNAP fusions and introduced these alleles at the native kinB locus on the chromosome of P. aeruginosa. Carboxy-terminal tagging of KinB with SNAP does not interfere with its function as the strain carrying kinB-SNAP forms biofilms that are indistinguishable from those of WT PA14 (Fig S3C and D). The KinB^{P390S}-SNAP protein is also produced and stable (Fig S3C), however, identical to the $\Delta kinB$ mutant, the strain carrying $kinB^{P390S}$ -SNAP fails to form biofilms (Fig S3D). These data demonstrate that KinB acts as a phosphatase to inhibit AlgB function $in\ vivo$. We therefore hypothesize, and we come back to this point below, that some other HK must phosphorylate AlgB to activate it and enable it to function as a repressor of biofilm development.

Our data show that the KinB-AlgB TCS functions downstream of RhIR to repress biofilm formation. An obvious mechanism by which RhIR could influence KinB-AlgB activity is by activating transcription of the *algB-kinB* operon. Indeed, RT-PCR shows that *algB-kinB* transcript levels are ~4-fold higher in the WT than in the $\Delta rhIR$ mutant (Fig 2D). Thus, RhIR activates expression of *algB-kinB* operon. By contrast, deletion of *kinB* has no effect on *rhIR* transcript levels (Fig 2E), confirming their epistatic relationship.

KinB has been reported to be required for pyocyanin production [24]. Pyocyanin is a RhIR-dependent virulence factor [21,31]. Our findings of a regulatory connection between KinB and RhIR suggest that KinB and RhIR could jointly regulate pyocyanin production. To test this idea, we measured pyocyanin production in planktonic cultures of WT, $\Delta rhIR$, $\Delta kinB$, and $\Delta rhIR$ $\Delta kinB$ strains. Similar to what has been reported previously, deletion of rhIR and/or kinB abolished pyocyanin production (Fig 2F). Overexpression of rhIR in the $\Delta rhIR$ strain and overproduction of kinB in the $\Delta kinB$ strain restored pyocyanin production, demonstrating that our expression constructs are functional (Fig 2F). By contrast, overexpression of either rhIR or kinB in the $\Delta rhIR$ $\Delta kinB$ double mutant failed to rescue pyocyanin production (Fig 2F). Thus, RhIR and KinB are both required activators of pyocyanin production in PA14. Consistent with AlgB

functioning as the RR for KinB, inactivation of AlgB (i.e., $algB^{STOP}$) in the $\Delta kinB$ background restored WT levels of pyocyanin production while overexpression of AlgB in the WT and the $algB^{STOP}$ mutant reduced pyocyanin levels (Fig 2F). Lastly, unlike WT AlgB, overexpression of AlgB^{D59N} failed to repress pyocyanin production suggesting that phosphorylation of AlgB is required for AlgB activity (Fig 2F).

To further explore the role of the KinB-AlgB TCS on RhIR-driven gene expression, we quantified expression of four other RhIR-activated genes [21]: hsiC2 (type-VI secretion), hcnA (hydrogen cyanide synthase), lecA (galactose-binding lectin), and lecB (fucose-binding lectin), all encoding virulence factors, in the WT and the $\Delta kinB$ mutant. Expression of all four genes was lower in the $\Delta kinB$ mutant than in the WT (Fig 2G). Introduction of the $algB^{STOP}$ mutation into the $\Delta kinB$ mutant restored expression of all four virulence genes to WT levels (Fig 2G). Thus, both RhIR and KinB activate virulence gene expression in P. aeruginosa. Moreover, we conclude that AlgB is epistatic to KinB for all the phenotypes tested here, and thus KinB and AlgB function in the same pathway, albeit in opposing manners, to control biofilm formation and virulence factor production.

The bacteriophytochrome BphP is the HK required to activate AlgB to mediate repression of quorum-sensing-controlled behaviors. We have invoked the existence of a putative HK to activate AlgB via phosphorylation. To identify this component, we used genetic suppressor analysis reasoning that mutants with defects in the upstream component required to phosphorylate AlgB would render AlgB non-functional. We further reasoned that such suppressor mutants would transform the $\Delta kinB$ smooth colony biofilm phenotype back to the rugose phenotype because in such mutants, AlgB could not act as a repressor of biofilm formation. We isolated 12 spontaneously-arising rugose mutants from $\Delta kinB$ smooth colony biofilms and analyzed them by whole genome sequencing (Fig 3A). Eight suppressors

contained deletions or missense mutations in the algB gene, while the remaining four suppressors harbored mutations in the bphP gene (Fig 3B, Table S2). bphP is located in a dicistron immediately downstream of bphO (Fig 3B, S1) [32]. We discuss bphO below; here we focus on bphP. Exactly analogous to mutation of algB, mutation of bphP was epistatic to kinB for all of the phenotypes tested. Specifically, engineering a STOP codon in place of the codon specifying residue 50 in the bphP gene showed no effect in WT PA14, but it restored biofilm formation, pyocyanin production, and virulence gene expression to the $\Delta kinB$ mutant (Fig 3C, D, and 2G). Consistent with BphP being required to activate AlgB, unlike in the WT, in the bphPSTOP mutant, overexpression of alaB failed to repress biofilm formation and pyocyanin production (Fig 3C, D). Furthermore, while overexpression of bphP in the WT reduced pyocyanin production to the levels of the $\triangle kinB$ mutant, overexpression of bphP had no effect in the algB^{STOP} mutant (Fig 3D). There is a severe growth defect associated with the overexpression of bphP. For this reason, in Fig 3D, rather than using plasmid pUCP18, we expressed bphP from the low copy number plasmid pBBR1-MCS5. Unfortunately, the presence of the empty pBBR-MCS5 plasmid in WT and mutant PA14 strains abrogates biofilm formation, so we could not perform the companion biofilm assay to test overexpression of bphP. Nonetheless, we can conclude from Fig 3C and 3D that BphP is necessary and sufficient to activate AlgB.

223

224

225

226

227

228

229

230

231

232

233

234

235

236

237

238

239

240

241

242

243

244

245

246

247

BphP is a bacteriophytochrome that assembles with its chromophore biliverdin, which is produced by the heme oxygenase BphO (Fig 3B, S1A and S1C) to generate a photo-sensing HK that is activated by light [32]. *P. aeruginosa* BphP contains the HDLRNPL motif that often contains the histidine residue that undergoes autophosphorylation in transmembrane HKs [33]. In *P. aeruginosa* BphP, this histidine is residue 513 (Fig S1C). To determine if BphP kinase activity is required for AlgB activation, we generated the *bphP*^{H513A} mutation, fused it to 3x*FLAG*, and introduced it onto the chromosome of the Δ*kinB* mutant. The BphP^{H513A}-3xFLAG protein is

produced and stable (Fig S3E), and identically to the $bphP^{STOP}$ allele, the $bphP^{H513A}$ mutation restored biofilm formation and pyocyanin production to the $\Delta kinB$ mutant (Fig 3C, D). Moreover, overexpression of algB in the $bphP^{H513A}$ mutant failed to repress biofilm formation and pyocyanin production (Fig 3C, D). These results show that BphP H513 and AlgB D59 are required for signal transmission, and the signal is presumably phosphorylation.

To assess phospho-relay between BphP and AlgB, we used our 3xFLAG-AlgB *in vivo* construct. In addition to introducing it into the chromosome of WT PA14, we engineered it onto the chromosome of the *bphP*^{STOP} mutant. Consistent with BphP being the kinase for AlgB, Fig 2C shows that the Δ*kinB bphP*^{STOP} mutant lacks the band corresponding to AlgB~P. These data suggest that BphP transfers phosphate to AlgB. To verify this finding, we performed *in vitro* phospho-transfer assays. We purified recombinant BphP and formed a complex with it and commercially-available biliverdin (BV) to obtain the BphP-BV chromoprotein. Upon incubation with radiolabeled ATP under ambient light, BphP-BV underwent autophosphorylation (Fig 3E). BphP-BV readily transferred radiolabeled phosphate to purified AlgB but not to AlgB^{D59N} (Fig 3E, S4). Purified BphP^{H513A} complexed with BV failed to autophosphorylate and thus could not transfer phosphate to AlgB (Fig S4A). Together, these data show that BphP-BV phosphorylates and thereby activates AlgB.

Our data suggest that KinB dephosphorylates AlgB while BphP phosphorylates AlgB. To directly test this hypothesis, we reconstituted the BphP-AlgB-KinB phosphorelay *in vitro*. We purified the recombinant KinB and KinB^{P390S} proteins and added them separately, at equimolar concentration, to AlgB~P pre-phosphorylated by BphP-BV. Fig 3F shows that over time, KinB dephosphorylates AlgB while AlgB~P levels remain unchanged in the presence of KinB^{P390S}. As control experiments, we added either KinB or KinB^{P390S} to AlgB in the presence of ATP but in the absence of BphP-BV. Both KinB and KinB^{P390S} underwent autophosphorylation and transferred phosphate to AlgB *in vitro*, but only WT KinB acted as a phosphatase to dephosphorylate AlgB

(Fig S5A-D). Although our findings show that KinB is a dual kinase/phosphatase, under our *in vivo* conditions, only KinB phosphatase activity was detected. Perhaps KinB can function as a kinase for AlgB when its stimulus is present (Fig 1). Identifying the natural signal that drives the KinB kinase activity is the subject of our future work. We conclude that BphP-AlgB-KinB forms a "three-component" system in which the RR AlgB is activated by the kinase activity of the HK BphP and inhibited by the phosphatase activity of the HK KinB.

279

280

281

282

283

284

285

286

287

288

289

290

291

292

293

294

295

296

297

273

274

275

276

277

278

BphP-mediated photo sensing represses P. aeruginosa quorum-sensing-controlled behaviors. The P. aeruginosa BphP bacteriophytochrome has been studied in vitro and its kinase activity is reported to be activated by light [32]. To explore whether BphP photo sensing has any effect on AlgB-controlled group behaviors in vivo, we compared biofilm formation by WT, $\triangle kinB$, $\triangle kinB$ bph P^{STOP} , and $\triangle kinB$ alg B^{STOP} PA14 strains in the dark and under different light conditions. We note that all of the biofilm experiments in the previous sections were performed under ambient light. First, we consider WT PA14 and the $\Delta kinB$ mutant in the no light condition. Fig 4A shows that, in the dark, both strains formed biofilms that were indistinguishable from one another. We interpret these results to mean that in the absence of light, the BphP kinase is inactive in both WT PA14 and the $\Delta kinB$ mutant, AlgB is not phosphorylated, so it too is inactive, and thus, no repression of biofilm formation occurs (Fig 1). Now we address the results under ambient light. WT PA14 formed biofilms but the $\Delta kinB$ strain did not (Fig 4A). Our interpretation is that, in the WT, ambient light activates the BphP kinase and phosphotransfer to AlqB occurs. However, the opposing KinB phosphatase activity strips the phosphate from AlgB, thereby eliminating AlgB-dependent repression of biofilm formation. Thus, WT PA14 forms biofilms under ambient light. In the case of the ∆kinB mutant, since there is no KinB phosphatase present, ambient light is sufficient to drive BphP-mediated phosphorylation of AlgB, AlgB~P accumulates, and it represses biofilm formation. Based on

these results, we infer that the presence or absence of light can alter group behaviors such as biofilm formation in *P. aeruginosa*.

298

299

300

301

302

303

304

305

306

307

308

309

310

311

312

313

314

315

316

317

318

319

320

321

322

Ambient light is a composite of different wavelengths of light. The PA14 BphP bacteriophytochrome is reported to be a far-red light sensing HK in vitro [20]. We wondered if a particular wavelength of light could maximally activate the BphP kinase activity in vivo, and if so, perhaps, under that condition, the BphP kinase activity could override the KinB phosphatase, enabling light to repress biofilm formation in WT PA14. To test this notion, we exposed PA14 strains to blue, red, and far-red light and monitored biofilm formation. In contrast to WT PA14, the $\Delta kinB$ mutant failed to form biofilms under blue and red light, suggesting that BphP is a promiscuous photoreceptor that is activated by blue and red light (Fig 4A). Indeed, BphP phosphorylates AlgB in vitro under ambient (as above), blue, red, and far-red light but it does not do so in the absence of light (Fig 4B). Importantly, when WT PA14 was exposed to far-red light, it failed to make biofilms, but rather, exhibited the smooth phenotype identical to the $\Delta kinB$ mutant (Fig 4A). We conclude that far-red light is the preferred wavelength for BphP and is sufficient to repress biofilm formation in WT P. aeruginosa. Finally, we show that light-mediated repression of biofilm formation requires functional BphP and AlgB as both the ΔkinB bphP^{STOP} and \(\Delta kinB \) algB\(STOP \) mutants did not repress biofilm formation under the conditions tested (Fig. 4A).

One mechanism by which light could suppress biofilm formation via BphP-AlgB is by decreasing the production of the Pel exopolysaccharide. To quantify the effect of light on *pel* expression, and in turn, on biofilm formation, we measuerd *pelA* transcript levels using quantitative RT-PCR analyses of WT, $\Delta kinB$, $\Delta kinB$ $algB^{STOP}$, and $\Delta kinB$ $bphP^{STOP}$ biofilms in darkness and under ambient and far-red light (Fig 4C). We used *rpoD* transcription as the control. Expression of *rpoD* did not change under any condition tested. Regarding *pelA*, analogous to what occurred for biofilm formation, there was no significant difference in *pelA*

expression between the WT and the $\Delta kinB$ strain in the dark, whereas transcription of pelA was ~14-fold lower in the $\Delta kinB$ strain than in the WT under ambient light. Repression of pelA expression depended on functional BphP and AlgB as the $\Delta kinB$ $bphP^{STOP}$ and $\Delta kinB$ $algB^{STOP}$ mutants transcribed pelA at high levels under both conditions. We conclude that dephosphorylation of AlgB does not occur in the $\Delta kinB$ mutant under ambient light. In this condition, BphP phosphorylates AlgB and AlgB~P represses biofilm formation via down-regulation of pelA expression. Lastly, in the WT, pelA transcript levels were ~4-fold lower under far-red light than in darkness. Therefore, far-red light is the strongest activator of BphP such that under far-red light, but not ambient light, the kinase activity of BphP overrides the phosphatase activity of KinB in the WT to drive AlgB~P accumulation, repression of pelA expression, and consequently, repression of biofilm formation.

In Fig 2, we showed that BphP is required for AlgB-dependent repression of virulence gene expression. Our results in Fig 4 suggest that light, by controlling BphP-dependent phosphorylation of AlgB, could control virulence in *P. aeruginosa*. To explore this idea further, we quantified the expression of the virulence-associated genes, *hsiC2*, *hcnA*, *lecA*, and *lecB* in biofilms of WT PA14 and in the Δ*kinB*, Δ*kinB algB*^{STOP}, and Δ*kinB bphP*^{STOP} strains under darkness, ambient light, and far-red light. The results mirror those for biofilm formation and *pelA* transcription. Only in the absence of the opposing KinB phosphatase activity is ambient light sufficient to activate BphP, whereas far-red light-driven BphP kinase activity can override the KinB phosphatase activity allowing accumulation of AlgB~P to levels that repress virulence gene expression. Again, light-mediated repression of virulence genes requires functional BphP and AlgB (Fig 4D). We conclude that BphP-dependent photo sensing represses virulence gene expression in *P. aeruginosa*.

Light possess both color (wavelength) and intensity properties. Above, we demonstrated that BphP can detect blue, red, and far-red light. To explore the possibility that *P. aeruginosa*

BphP is also capable of detecting light intensity, we varied the intensity of far-red light since it has the most dramatic effect on PA14 phenotypes. We used repression of biofilm formation as the readout. Biofilm formation decreased with increasing intensity of far-red light in the WT and $\Delta kinB$ mutant but remained unaltered in the bphP^{STOP} mutant (Fig 5A). The highest intensity of light we tested (bottom-most panel in Fig 5A) is similar to that present in natural sunlight (5.5 W/m² in a 5 nm window around 730 nm; ASTM G173-03 Reference Solar Spectra, www.astm.org). At this intensity, WT biofilm formation was maximally repressed showing that BphP kinase dominates over KinB phosphatase. The $\Delta kinB$ mutant generates suppressor flares under this condition, suggesting that one role of the KinB phosphatase is to keep the BphP kinase activity in check. To verify that far-red light specifically altered biofilm behavior without affecting general physiology, we quantified rpoD and pelA transcript levels in the WT and bphP^{STOP} mutant biofilm samples grown under the different light intensities (Fig 5B). Expression of rpoD did not change under any condition tested, while transcription of pelA decreased progressively in the WT with increasing intensity of far-red light. At the highest intensity of farred light tested, expression of pelA was ~12-fold lower than that in the bphPSTOP mutant that cannot convey the light cue internally to AlgB. These results demonstrate that P. aeruginosa biofilm formation can be modulated simply by tuning the intensity of far-red light in which the strain is grown.

366

367

368

369

370

371

372

365

348

349

350

351

352

353

354

355

356

357

358

359

360

361

362

363

364

The BphP-AlgB phosphorelay is conserved in diverse bacteria. BphP bacteriophytochromes are a major class of photoreceptors widely distributed in non-photosynthetic bacteria [14]. These BphP HKs either lack a partner RR, or when they are co-transcribed with a cognate RR gene, the physiological output of the circuit is unknown. Thus, the downstream signaling components and consequences of photo sensing in non-photosynthetic bacteria are not understood. Our discovery of AlgB as the cognate RR for the

orphan light sensing BphP HK in a non-photosynthetic bacterium, coupled with our demonstration of the biofilm and virulence outputs of photo sensing, puts us in a position to test the generality of our findings. As a first step, we generated a phylogenetic tree containing 150 BphP orthologs that are the closest homologs to *P. aeruginosa* BphP (Fig 6A, S6). The majority of these BphP orthologs are present in non-photosynthetic bacteria from diverse phyla. The Pseudomonads fall into discrete clusters hinting at acquisition of BphP via horizontal gene transfer. With respect to AlgB and KinB, we find that, while KinB is present only in the Pseudomonads, *Acinetobacter baumannii*, and *Enterobacter cloacae* (Fig 6A, S1, S6), AlgB is present in ~93% of the bacterial species in our BphP-based phylogenetic tree (Fig 6A, S5). We note that in all of the bacteria that do not encode AlgB, for example, *Deinococcus* spp., BphR is the cognate RR for BphP (Fig 6A, S1, 2, 5, and [32]). None of these *bphP*-encoding bacteria possesses both BphR and AlgB. Therefore, the pattern that emerges is that BphB is widely distributed in non-photosynthetic bacteria and the cognate RR is either AlgB or BphR.

To test if BphP can interact with and phosphorylate AlgB in bacteria other than P. aeruginosa, we purified AlgB orthologs from diverse Proteobacteria: Rhodospirillum centenum (α), Achromobacter xylosoxidans (β) and Pseudomonas putida (γ) (Fig S2). We incubated these AlgB proteins with an equimolar concentration of autophosphorylated P. aeruginosa BphP-BV. Phosphotransfer from BphP-BV to the AlgB orthologs occurred in all cases, albeit to varying degrees (Fig 6B). To eliminate the possibility that BphP-BV is a promiscuous kinase for NtrC family RRs, we purified NtrC from P. aeruginosa and incubated with autophosphorylated BphP-BV. BphP-BV failed to phosphorylate NtrC (Fig 6B). We conclude that BphP is the specific HK for AlgB, and AlgB appears to have a conserved function in photosensory signal transduction in diverse bacteria.

DISCUSSION

Our study reveals that the non-photosynthetic pathogenic bacterium *P. aeruginosa* detects and responds to light to repress group behaviors including virulence factor production and biofilm formation. The photoreceptor BphP functions as a light-activated HK that phosphorylates the AlgB RR. AlgB~P represses group behaviors but is antagonized by its canonical HK KinB. Specifically, KinB dephosphorylates AlgB, and thus, KinB functions as an activator of group behaviors. Our work shows that AlgB functions as a hub protein that has three inputs -- quorum sensing via RhIR, photo sensing via BphP, and an unknown signal via KinB. While quorum sensing activates *algB* expression, photo sensing activates AlgB function, and thus the presence or absence of light can override the quorum-sensing input from RhIR. We reason that, at high cell density, RhIR will drive AlgB production. However, if there is no light, BphP will not phosphorylate and activate AlgB. In turn, AlgB will not repress group behaviors. To our knowledge, the BphP-AlgB photosensory signal transduction cascade represents the first example of light-mediated control of group behaviors in the global pathogen *P. aeruginosa*.

Light is a ubiquitous source of energy that drives the anabolic process of photosynthesis in photosynthetic organisms. However, the wide distribution of photoreceptors in all domains of life suggests roles for photo sensing in behaviors far beyond photosynthesis. Plants, for example, use light cues to regulate activities such as seed germination [34], stomatal opening [35], and defenses against microbes [36–38]. Furthermore, plant vascular systems can function as bundles of optical fibers to efficiently transmit light, particularly far-red light, that is not absorbed by plant pigments, allowing opportunities for photo sensing in roots and possibly in the rhizosphere [39]. Many of the *bphP*-encoding bacteria from the phylogenetic tree in Fig 6A that also possess AlgB, are members of the rhizosphere microbiome [40]. Perhaps these non-photosynthetic bacteria exploit light cues to colonize and/or to fine-tune their mutualistic or pathogenic interactions with their plant hosts as well as adjust their physiology in the rhizosphere. While we do not know the evolutionary forces that drove *P. aeruginosa* to become

a photo-sensing bacterium, we speculate below on possible advantages *P. aeruginosa* could accrue by detecting light in the environment and in the human host.

Light provides spatial and temporal information to higher organisms. Does light serve a similar purpose in bacteria? Recent studies have reported that BphP plays a role in multiple stages of infection by the foliar plant pathogens *Xanthomonas campestris pv. campestris* and *Pseudomonas syringae pv. syringae* [41] [42], in each case, via an unknown but putative downstream RR. Based on our phylogenetic analysis, we speculate that AlgB fulfils this role. We further speculate that *P. aeruginosa*, which is a plant pathogen [43], responds to light cues via the BphP-AlgB TCS to appropriately modulate its biofilm and virulence programs, particularly, to inhibit virulence during daylight enabling avoidance of plant defense mechanisms. For instance, during the day, chlorophyll in leaves removes most of the red wavelength from sunlight but little of the far-red spectrum [44]. Thus, far-red light is readily available, and based on our work here, could signal to *P. aeruginosa* to tamp down virulence factor production and biofilm formation, allowing it to optimize those programs in line with host conditions as shaded leaves are more susceptible to infection than leaves exposed to direct light [45].

In addition to providing spatial-temporal information, light can also reveal other key parameters to which bacteria respond. Detection of blue light via LOV and BLUF domain proteins modulates general stress responses in some non-photosynthetic bacteria such as *Bacillus subtilis* and *Caulobacter crescentus* [46,47]. Light, through the LOV-HK of the mammalian pathogen *Brucella abortus* is crucial for virulence in a macrophage infection model, although the components connecting light to the virulence response remain undefined. It is also proposed that *B. abortus* uses light as an indicator of whether it is inside or outside of its animal host [48]. The *P. aeruginosa* genome does not encode LOV or BLUF domain proteins [11]. *P. aeruginosa*, possesses only one identifiable photoreceptor, BphP. Nonetheless, we showed that *P. aeruginosa* is capable of detecting blue, red, and far-red light via BphP (Fig 4A, B). Perhaps,

an advantage of BphP promiscuity is that it enables detection of higher energy, and therefore, phototoxic blue light, in addition to the lower energy but highly penetrative far-red light. Such a scenario would endow *P. aeruginosa* with the plasticity to diversify its physiological outputs in response to particular wavelengths of light, without the necessity of a distinct photoreceptor for each wavelength.

451

452

453

454

455

456

457

458

459

460

461

462

463

464

465

466

467

468

469

470

471

472

473

474

475

476

An advantage P. aeruginosa could accrue by sensing light on or within a mammalian host would be the ability to tune into the host circadian rhythm and its associated responses. Circadian clocks influence various aspects of health and disease such as sleep/wake cycles and metabolism [49] [50]. Disruption of circadian rhythms are associated with fitness costs [50]. In mammals, both innate and adaptive immune responses are controlled by the circadian clock such that the immune system is primed to combat pathogens during the host active phase while immune functions undergo regeneration and repair during the resting phase of the daily cycle. Parasites such as *Plasmodium* spp. that cause malaria, synchronize their replication cycle with host circadian rhythms for optimized infection and dissemination [51]. Likewise, viruses such as Herpes and Influenza A have been shown to exploit the mammalian circadian clock for their own gain i.e., to successfully avoid host immune responses enabling maximal replication [52] [53]. Perhaps, P. aeruginosa uses light as a signal that reveals when the host immune response is at peak function, and accordingly, at that time, P. aeruginosa represses biofilm formation and virulence factor expression as a mechanism that enhances evasion of host defenses. If so, a human host infected with P. aeruginosa during the night would be colonized to higher levels, compared to a host acquiring an infection during the day. Synchronizing infectivity with light/dark cues to enable optimal infection could be a common feature of non-photosynthetic photoreceptor-harboring pathogens.

P. aeruginosa is a priority pathogen on the CDC (Centers for Disease Control and Prevention) ESKAPE pathogen list (a set of bacteria including Enterococcus faecium, Staphylococcus aureus, Klebsiella pneumoniae, Acinetobacter baumannii, P. aeruginosa and

Enterobacter spp. that are designated as multi-drug resistant pathogens requiring new antimicrobials for treatment), and a critical pathogen on the WHO (World Health Organization) priority list [54,55]. Our phylogenetic analysis suggests that the KinB-AlgB-BphP module is conserved in the genomes of *A. baumannii* and Enterobacter cloacae, perhaps acquired from *P. aeruginosa* via horizontal gene transfer, as the AlgB primary sequence is nearly identical between the three species. We speculate that, beyond *P. aeruginosa*, BphP-AlgB-dependent photo sensing also affects the physiology, and possibly the virulence of these ESKAPE pathogens. Collectively, the results from this study provide unanticipated insight into *P. aeruginosa* physiology and a surprising possibility for therapeutic intervention—shining light on a deadly and actively studied pathogen, *P. aeruginosa*, to attenuate virulence and biofilm formation. One can imagine such a strategy could be deployed in external infections such as burns, which are highly susceptable *P. aeruginosa* and could, moreover, be subjected to precise light regimes.

492 493	ACKNOWLEDGEMENTS
494	We thank Wei Wang and the Genomics Core Facility at Princeton University for help with whole
495	genome sequencing. We thank Ned Wingreen, Anne-Florence Bitbol, Joseph E. Sanfillipo, and
496	all members of the Bassler group for thoughtful discussions. This work was supported by the
497	Howard Hughes Medical Institute, NIH Grant 5R37GM065859, and National Science foundation
498	Grant MCB-1713731 to B.L.B., and a NIH Grant 1K99GM129424-01 to S.M.
499	
500	AUTHOR CONTRIBUTIONS
501	S.M., V.S. and M.J. conducted experiments; S.M. and M.T. analyzed data; S.M., M.J. and
502	B.L.B. designed the experiments; S.M. and B.L.B. wrote the paper.
503	
504	DECLARATION OF INTERESTS
505	The authors declare no competing interests.

MATERIALS AND METHODS

509 Bacterial strains and growth conditions. All strains and plasmids used in this study are listed 510 in Supplemental Tables S3 and S4, respectively. P. aeruginosa PA14 and mutants were grown at 37°C in lysogeny broth (LB) (10 g tryptone, 5 g yeast extract, 5 g NaCl per L), in 1% Tryptone 511 512 broth (TB) (10 g tryptone per L), or on LB plates fortified with 1.5% Bacto agar. When 513 appropriate, antimicrobials were included at the following concentrations: 400 µg/mL carbenicillin, 30 μg/mL gentamycin, and 100 μg/mL irgasan. Escherichia coli was grown at 37°C 514

in LB, or on LB plates fortified with 1.5% Bacto agar and the following concentrations of

antimicrobials as appropriate: 15 µg/mL gentamycin, 50 µg/mL kanamycin, and 100 µg/mL

ampicillin. Isopropyl β-D-thiogalactopyranoside (IPTG, Sigma) was added to the medium at the

indicated concentrations when appropriate.

519

520

521

522

523

524

525

526

527

528

529

530

531

532

518

515

516

517

507

508

Mutant strain and plasmid construction. Strains and plasmids were constructed as described previously [21]. Briefly, to construct marker-less in-frame chromosomal deletions and substitutions in PA14, DNA fragments flanking the gene of interest were amplified, assembled by the Gibson method [56], and cloned into suicide vector pEXG2 [57]. The resulting plasmids were used to transform E. coli SM10λpir, and subsequently, mobilized into PA14 strains via biparental mating. Exconjugants were selected on LB containing gentamicin and irgasan, followed by recovery of deletion mutants on LB medium containing 5% sucrose. Candidate mutants were confirmed by PCR and Sanger sequencing. Transposon insertions in the PA14 chromosome were generated by mating the PA14 ΔrhlR parent strain with E. coli SM10λpir harboring pIT2 (ISlacZ/hah) [23]. Insertion mutants were selected on LB agar containing 60 μg/mL tetracycline and 100 μg/mL irgasan was included in the agar to counter select against the E. coli donor. Transposon insertion locations were determined by arbitrary PCR and sequencing as described previously [23].

Protein production constructs were generated by amplifying the *algB*, *kinB*, and *bphP* coding regions and cloning them in pET28b or pET21b expression vectors (Novagen) to obtain pET28b-His6-AlgB, pET21b-KinB-His6, and pET21b-BphP-His6, respectively. To generate the AlgB^{D59N}, KinB^{P390S}, and BphP^{H513A} variants, the corresponding mutations were engineered on to the pET28b-His6-AlgB, pET21b-KinB-His6, and pET21b-BphP-His6 plasmids, respectively, via Gibson assembly. AlgB orthologs from *R. centenum* (Rce) and *A. xylosoxidans* (Axy) were amplified from gene fragments obtained from Integrated DNA Technologies, and that from *P. putida* (Ppu) was amplified from the *P. putida* KT2440 genome. All of the gene orthologs were cloned into the pET28b plasmid.

Pyocyanin assay. PA14 strains were grown overnight in LB liquid medium at 37° C with shaking at 250 rotations per minute (rpm). The cells were pelleted by centrifugation at 21,130 x g for 2 min and the clarified supernatants were passed through 0.22 μ m filters (Millipore) into clear plastic cuvettes. The OD₆₉₅ of each sample was measured on a spectrophotometer (Beckman Coulter DV 730) and normalized to the culture cell density which was determined by OD₆₀₀.

Colony biofilm assay. The procedure for establishing colony biofilms has been described [21]. Briefly, 1 μ L of overnight cultures of PA14 strains were spotted onto 60 x 15 mm Petri plates containing 10 mL 1% TB medium fortified with 40 mg/L Congo red and 20 mg/L Coomassie brilliant blue dyes and solidified with 1% agar. Biofilms were grown at 25°C for 72 h in an incubator (Benchmark Scientific) and images were acquired using a Leica stereomicroscope M125 mounted with a Leica MC170 HD camera at 7.78x zoom.

For biofilms exposed to specific wavelengths of light, the following light-emitting diodes (LED) were used: blue – 430 nm (Diffused RGB LED, #159, Adafruit), red – 630 nm (Diffused RGB LED, #159, Adafruit), and far-red – 730 nm (LST1-01G01-FRD1-00, Opulent). Ambient

light exposure refers to biofilms grown under laboratory light conditions. For the biofilms shown in Fig 4A, light intensity was normalized by photon flux and the following intensities were used: blue (0.7 W/m²), red (1 W/m²), and far-red (1.1 W/m²). Light intensity was calibrated using a laser power meter (Ophir) in a 5 nm window at the appropriate wavelength. Biofilm samples were grown in custom laser-cut acrylic chambers. Each chamber housed a single LED light source and an individual petri plate containing 4 technical replicates. Samples exposed to darkness were housed in the same chambers as the light-exposed samples, but with no current applied to the LEDs.

qRT-PCR. WT PA14 and mutant strains were harvested from planktonic cultures (OD₆₀₀ = 1.0) or from biofilms grown for 72 h. RNA was purified using the Zymo Research kit, and the preparations were subsequently treated with DNAse (TURBO DNA-free™, Thermo Fisher). cDNA was synthesized using SuperScript® III Reverse Transcriptase (Invitrogen) and quantified using PerfeCTa® SYBR® Green FastMix® Low ROX (Quanta Biociences).

Protein purification. His6-AlgB. The pET28b-His6-AlgB protein production vector was transformed into *E. coli* BL21 (DE3) and the culture grown to ~0.8 OD₆₀₀ in 1 L of LB supplemented with 50 μg/mL kanamycin at 37°C with shaking at 220 rpm. Protein production was induced by the addition of 1 mM IPTG, followed by incubation of the culture for another 3 h at 25°C with shaking. The cells were pelleted by centrifugation at 16,100 x g for 20 min and resuspended in AlgB-lysis buffer [50 mM NaH₂PO₄ pH 8.0, 300 mM NaCl, 1 mM MgCl₂, 1 mM DTT, 5% glycerol, 0.1% Triton X-100, 10 mM Imidazole, and protease inhibitor cocktail (Roche)]. The preparation was frozen at -80°C overnight. The frozen cell pellet was thawed on ice and the cells lysed by sonication (1 s pulses for 15 s). The sample was subjected to centrifugation at 32,000 x g for 30 min at 4°C. The resulting clarified supernatant was combined with Ni-NTA resin (Novagen) and incubated for 3 h at 4°C. The bead/lysate mixture was loaded

onto a 1 cm separation column (Bio-Rad), the resin was allowed to pack, and then it was washed with AlgB-wash buffer [50 mM NaH₂PO₄ pH 8.0, 300 mM NaCl, 1 mM MgCl₂, 1 mM DTT, 5% glycerol, 0.1% Triton X-100, 30 mM Imidazole, and protease inhibitor cocktail (Roche)]. Resin-bound His6-AlgB was eluted twice with 1 mL AlgB-wash buffer containing 250 mM Imidazole. Fractions were analyzed by SDS-PAGE and the gel was stained with Coomassie Brilliant Blue to assess His6-AlgB purity. Purified protein was dialyzed in AlgB-storage buffer [50 mM NaH₂PO₄ pH 8.0, 300 mM NaCl, 1 mM MgCl₂, 1 mM DTT, 5% glycerol, and 0.1% Triton X-100], and stored at -80°C.

BphP-His6. The pET21b-BphP-His6 protein production vector was transformed into *E. coli* BL21-CodonPlus (DE3)-RIPL (Agilent Technologies). BphP-His6 was purified as described for His6-AlgB with the following changes in buffers: BphP-lysis buffer [50 mM NaH₂PO₄ pH 8.0, 300 mM NaCl, 1% Triton X-100, 0.1% β-mercaptoethanol, 10 mM Imidazole, and protease inhibitor cocktail (Roche)], BphP-wash buffer [50 mM NaH₂PO₄ pH 8.0, 300 mM NaCl, 1% Triton X-100, 0.1% β-mercaptoethanol, 30 mM Imidazole, and protease inhibitor cocktail (Roche)], and BphP-storage buffer [50 mM NaH₂PO₄ pH 8.0, 300 mM NaCl, 1% Triton X-100, 0.1% β-mercaptoethanol, 5% glycerol].

KinB-His6. The pET21b-KinB-His6 protein production vector was transformed into *E. coli* BL21 (DE3). KinB-His6 protein was purified exactly as described above for BphP-His6.

Phosphorylation assays. Autophosphorylation assays were performed with purified WT BphP and the BphP^{H513A} variant or with KinB and the KinB^{P390S} variant. 100 μM BphP or BphP^{H513A} was incubated under ambient light with 10-fold molar excess of Biliverdin (Sigma-Aldrich) for 1 h prior to the assay to form the light-activated BphP-BV stocks. Reactions were carried out in phosphorylation buffer [50 mM Tris pH 8.0, 100 mM KCl, 5 mM MgCl₂, and 10% (v/v) glycerol],

and were initiated with the addition of 100 μ M ATP and 2 μ Ci [γ - 32 P]-ATP (Perkin Elmer). Reactions were incubated at room temperature and terminated by the addition of SDS-PAGE loading buffer. Reaction products were separated using SDS-PAGE. Gels were dried at 80°C on filter paper under vacuum, exposed to a phosphoscreen overnight, and subsequently analyzed using a Typhoon 9400 scanner and ImageQuant software. For phosphotransfer to AlgB, an equimolar concentration of AlgB was added to the phospho-BphP-BV or phospho-KinB proteins. Reactions were incubated at room temperature for the indicated times and terminated by the addition of SDS-PAGE loading buffer. For the BphP-AlgB phoshporelay shown in Fig S4B, BphP-BV was incubated under specific light wavelengths using the same devices as described above for colony biofilm assay.

Dephosphorylation of AlgB~P: 10 μ M AlgB was phosphorylated for 30 min in reactions containing 10 μ M BphP-BV, 100 μ M ATP, and 2 μ Ci [γ -32P]-ATP in phosphorylation buffer. Subsequently, the reactions containing AlgB~P were applied to gel filtration spin columns (Probe Quant G-50, GE healthcare) to remove ATP. Dephosphorylation reactions were initiated by adding 10 μ M KinB or KinB^{P390S}. Aliquots were taken at the indicated times and analyzed as described above.

Phos-Tag SDS-PAGE and Western Blotting. WT PA14 and mutant strains were harvested from planktonic cultures (OD₆₀₀ = 1.0). Cells were resuspended in 100 μl of ice-cold BugBuster reagent (Novagen) containing EDTA-free Protease Inhibitor Cocktail (Roche), followed by end-over-end rotation on a nutator at room temperature for 30 min. Cell debris was removed by centrifugation (4°C at 10,000 rpm for 1 min). 50 μL of 4x SDS-PAGE loading buffer (Thermo Fisher Scientific) containing 15% β-mercaptoethanol was combined with 50 μL of the sample supernatant. 10 μL of samples were loaded onto a 12.5% SuperSepTM Phos-tagTM gel (Wako Pure Chemical Industries). Samples were subjected to electrophoresis at 4°C for 3 h. Gels were

incubated for 20 min on a shaking platform in 1x transfer buffer containing 1 mM EDTA, and reequilibrated for 20 min in 1x transfer buffer lacking EDTA. Proteins were transferred to nitrocellulose membranes, blocked with 5% skim milk in TBS at room temperature for 1 h, and incubated with primary anti-FLAG antibody (Sigma Aldrich) at 1:5000 dilution in 5% skim milk in TBS overnight 4°C on a rocking platform. Membranes were washed three times with TBS-Tween 20 at room temperature for 10 min, on a rocking platform, and subsequently developed with SuperSignal West Femto Kit (Thermo Scientific) and captured with LAS-4000 Imager (GE Healthcare).

643

644

645

646

647

648

649

650

651

652

653

654

655

656

657

658

659

635

636

637

638

639

640

641

642

Whole genome sequencing. P. aeruginosa strains were harvested from planktonic cultures $(OD_{600} = 2.0)$ and DNA was purified using DNeasy Blood & Tissue kit (Qiagen). The Nextera DNA Library Prep kit (Illumina, CA) was employed with 2 ng of genomic DNA to prepare the library. Unique barcodes were added to each sample to enable multiplexing. The libraries were examined for quality using Bioanalyzer DNA High Sensitivity chips (Agilent, CA) and quantified using a Qubit fluorometer (Invitrogen, CA). DNA libraries from the different strains were pooled at equal molar amounts and sequenced using an Illumina MiSeq as pair-end 2x100 nt reads. Only the Pass-Filter (PF) reads were used for further analysis.

Whole-genome sequencing data were processed with breseg version 0.33.2 to identify mutations relative to the reference P. aeruginosa UCBPP-PA14 genome (www.pseudomonas.com; [58]). All high-confidence and putative SNPs and deletion events were confirmed by a manual examination of the read pileups with GenomeViewer IGV 2.4.8. A sample collected prior to the suppressor mutation screen was aligned against the reference genome of PA14, yielding a manually curated list of 25 differences acquired by our laboratory strain prior to the experiment (19 SNPs, 6 single-nucleotide indels). Applying these differences to PA14 using gdtools (part of the breseq package) yielded an updated reference genome against which all other samples were compared. Table S2 reports all high-confidence mutations
 identified in this analysis.

REFERENCES

664 665

- Flemming H, Wingender J. The biofilm matrix. Nat Rev Microbiol. 2010;8: 623–33. doi:10.1038/nrmicro2415
- Flemming HC, Wingender J, Szewzyk U, Steinberg P, Rice SA, Kjelleberg S. Biofilms: An emergent form of bacterial life. Nat Rev Microbiol. 2016;14: 563–575. doi:10.1038/nrmicro.2016.94
- Koo H, Allan RN, Howlin RP, Stoodley P, Hall-Stoodley L. Targeting microbial biofilms: Current and prospective therapeutic strategies. Nat Rev Microbiol. 2017;15: 740–755. doi:10.1038/nrmicro.2017.99
- 674 4. Dahlstrom KM, O'Toole GA. A Symphony of Cyclases: Specificity in Diguanylate Cyclase Signaling. Annu Rev Microbiol. 2017;71: 179–195. doi:10.1146/annurev-micro-090816-093325
- Giacalone D, Smith TJ, Collins AJ, Sondermann H, Koziol LJ, O'Toole GA. Ligand-mediated biofilm formation via enhanced physical interaction between a diguanylate cyclase and its receptor. MBio. 2018;9: 1–13. doi:10.1128/mBio.01254-18
- 680 6. Hammer BK, Bassler BL. Quorum sensing controls biofilm formation in *Vibrio cholerae*.
 681 Mol Microbiol. 2003;50: 101–114. doi:10.1046/j.1365-2958.2003.03688.x
- Mukherjee S, Bassler BL. Bacterial quorum sensing in complex and dynamically changing environments. Nat Rev Microbiol. 2019;17: 371–382. doi:10.1038/s41579-019-0186-5
- 8. Papenfort K, Bassler BL. Quorum sensing signal-response systems in Gram-negative bacteria. Nat Rev Microbiol. 2016;14: 576–88. doi:10.1038/nrmicro.2016.89
- 687 9. Miller MB, Skorupski K, Lenz DH, Taylor RK, Bassler BL. Parallel quorum sensing 688 systems converge to regulate virulence in *Vibrio cholerae*. Cell. 2002;110: 303–314. 689 doi:10.1016/S0092-8674(02)00829-2
- 690 10. Rutherford ST, Bassler BL. Bacterial Quorum Sensing: Its Role in Virulence and Possibilities for Its Control. Cold Spring Harb Perspect Med. 2012;2:a012427: 1–26.
- Horst MA Van Der, Key J, Hellingwerf KJ. Photosensing in chemotrophic, non-phototrophic bacteria: let there be light sensing too. Trends Microbiol. 2007;15: 554–562. doi:10.1016/j.tim.2007.09.009
- Kottke T, Xie A, Larsen DS, Hoff WD. Photoreceptors Take Charge: Emerging Principles for Light Sensing. Annu Rev Biophys. 2018;47: 291–313.
- 50. doi:10.1146/annurev-biochem-060614-034411
- 700 14. Gomelsky M, Hoff WD. Light helps bacteria make important lifestyle decisions. Trends Microbiol. 2011;19: 441–448. doi:10.1016/j.tim.2011.05.002
- 702 15. Gourinchas G, Etzl S, Winkler A. Bacteriophytochromes from informative model 703 systems of phytochrome function to powerful tools in cell biology. Curr Opin Struct Biol. 704 2019;57: 72–83. doi:10.1016/j.sbi.2019.02.005

- Beattie GA, Hatfield BM, Dong H, McGrane RS. Seeing the Light: The Roles of Red- and
 Blue-Light Sensing in Plant Microbes. Annu Rev Phytopathol. 2018;56: 41–66.
 doi:10.1146/annurev-phyto-080417-045931
- 708 17. Davies DG, Parsek MR, Pearson JP, Iglewski BH, Costerton JW, Greenberg EP. The 709 Involvement of Cell-to-Cell Signals in the Development of a Bacterial Biofilm. Science. 710 1998:280: 295–298. doi:10.1126/science.280.5361.295
- 711 18. Rumbaugh KP, Griswold JA, Hamood AN. The role of quorum sensing in the in vivo virulence of *Pseudomonas aeruginosa*. Microbes Infect. 2000;2: 1721–1731. doi:10.1016/S1286-4579(00)01327-7
- Ma S, Wozniak DJ, Ohman DE. Identification of the histidine protein kinase KinB in
 Pseudomonas aeruginosa and its phosphorylation of the alginate regulator AlgB. J Biol
 Chem. 1997;272: 17952–17960. doi:10.1074/jbc.272.29.17952
- 717 20. Tasler R, Moises T, Frankenberg-Dinkel N. Biochemical and spectroscopic 718 characterization of the bacterial phytochrome of *Pseudomonas aeruginosa*. FEBS J. 719 2005;272: 1927–1936. doi:10.1111/j.1742-4658.2005.04623.x
- Mukherjee S, Moustafa D, Smith CD, Goldberg JB, Bassler BL. The RhIR quorum-sensing receptor controls *Pseudomonas aeruginosa* pathogenesis and biofilm development independently of its canonical homoserine lactone autoinducer. PLoS Pathog. 2017;13: 1–25. doi:10.1371/journal.ppat.1006504
- 724 22. Mukherjee S, Moustafa DA, Stergioula V, Smith CD, Goldberg JB. The PqsE and RhlR 725 proteins are an autoinducer synthase – receptor pair that control virulence and biofilm 726 development in *Pseudomonas aeruginosa*. 2018;115: E9411–E9418. 727 doi:10.1073/pnas.1814023115
- Jacobs MA, Alwood A, Thaipisuttikul I, Spencer D, Haugen E, Ernst S, et al.
 Comprehensive transposon mutant library of *Pseudomonas aeruginosa*. 2003; 0–5.
- Chand NS, Lee JSW, Clatworthy AE, Golas AJ, Smith RS, Hung DT. The sensor kinase
 KinB regulates virulence in acute *Pseudomonas aeruginosa* infection. J Bacteriol.
 2011;193: 2989–2999. doi:10.1128/JB.01546-10
- 733 25. Chand NS, Clatworthy AE, Hung DT. The two-component sensor KinB acts as a phosphatase to regulate *Pseudomonas aeruginosa* Virulence. J Bacteriol. 2012;194: 6537–6547. doi:10.1128/JB.01168-12
- 736 26. Friedman L, Kolter R. Genes involved in matrix formation in *Pseudomonas aeruginosa* PA14 biofilms. Mol Microbiol. 2004;51: 675–690. doi:10.1046/j.1365-2958.2003.03877.x
- 738 27. Wozniak D, Wyckoff T, Starkey M, Keyser R, Azadi P, O'Toole G, et al. Alginate is not a significant component of the extracellular polysaccharide matrix of PA14 and PAO1
 740 *Pseudomonas aeruginosa* biofilms. Proc Natl Acad Sci U S A. 2003;100: 7907–12. doi:10.1073/pnas.1231792100
- 742 28. Ma S, Selvaraj U, Ohman DE, Quarless R, Hassett DJ, Wozniak DJ. Phosphorylation-743 independent activity of the response regulators AlgB and AlgR in promoting alginate 744 biosynthesis in mucoid *Pseudomonas aeruginosa*. J Bacteriol. 1998;180: 956–968.
- 745 29. Wozniak DJ, Ohman DE. *Pseudomonas aeruginosa* AlgB, a Two-Component Response Regulator of the NtrC Family, Is Required for algD Transcription. 1991;173: 1406–1413.

- 747 30. Bush M, Dixon R. The Role of Bacterial Enhancer Binding Proteins as Specialized 748 Activators of σ^{54} -Dependent Transcription. Microbiol Mol Biol Rev. 2012;76: 497–529. 749 doi:10.1128/MMBR.00006-12
- 31. Brint JM, Ohman DE. Synthesis of Multiple Exoproducts in *Pseudomonas aeruginosa* Is under the Control of RhIR-RhII, Another Set of Regulators in Strain PAO1 with Homology to the Autoinducer-Responsive LuxR-Luxl Family. 1995;177: 7155–7163.
- 753 32. Bhoo SH, Davis SJ, Walker J, Karniol B, Vierstra RD. Bacteriophytochromes are 754 photochromic histidine kinases using a biliverdin chromophore. Nature. 2001;414: 776– 755 779. doi:10.1038/414776a
- 33. Bhate MP, Molnar KS, Goulian M, Degrado WF. Signal Transduction in Histidine
 Kinases: Insights from New Structures. Struct Des. 2015;23: 981–994.
 doi:10.1016/j.str.2015.04.002
- 759 34. Mathews S. Phytochrome-mediated development in land plants : red light sensing 760 evolves to meet the challenges of changing light environments. 2006; 3483–3503. 761 doi:10.1111/j.1365-294X.2006.03051.x
- 35. Shimazaki K, Doi M, Assmann SM, Kinoshita T. Light Regulation of Stomatal Movement.
 Annu Rev Plant Biol. 2007;58: 219–47. doi:10.1146/annurev.arplant.57.032905.105434
- 36. Bhardwaj V, Meier S, Petersen LN, Ingle RA, Roden LC. Defence Responses of
 Arabidopsis thaliana to Infection by *Pseudomonas syringae* Are Regulated by the
 Circadian Clock. 2011;6: 1–8. doi:10.1371/journal.pone.0026968
- Neukermans J, Li S, Aro E, Noctor G, Kangasja S. Photosynthesis, photorespiration, and light signalling in defence responses. 2012;63: 1619–1636. doi:10.1093/jxb/err402
- 769 38. Roden LC, Ingle RA. Lights, Rhythms, Infection: The Role of Light and the Circadian Clock in Determining the Outcome of Plant Pathogen Interactions. 2009;21: 2546–2552. doi:10.1105/tpc.109.069922
- The second secon
- Duran P, Thiergart T, Garrido-oter R, Agler M, Kemen E, Schulze-lefert P, et al. Microbial
 Interkingdom Interactions in Roots Promote Arabidopsis Survival. Cell. 2018; 973–983.
 doi:10.1016/j.cell.2018.10.020
- HR, Toum L, Sycz G, Sieira R, Toscani AM, Gudesblat GE, et al. *Xanthomonas campestris* attenuates virulence by sensing light through a bacteriophytochrome photoreceptor . EMBO Rep. 2016;17: 1565–1577. doi:10.15252/embr.201541691
- 781 42. Wu L, McGrane RS, Beattie GA. Light Regulation of Swarming Motility in *Pseudomonas* 782 syringae Integrates Signaling Pathways Mediated by a Bacteriophytochrome and a LOV
 783 Protein. MBio. 2013;4: 1–9. doi:10.1128/mbio.00334-13
- 784 43. Starkey M, Rahme LG. Modeling *Pseudomonas aeruginosa* pathogenesis in plant hosts. 785 Nat Protoc. 2009;4: 117–124. doi:10.1038/nprot.2008.224
- 786 44. Smith H. Phytochromes and light signal perception by plants—an emerging synthesis. Nature. 2000;407: 585–591.

- de Wit M, Spoel SH, Sanchez-Perez GF, Gommers CM, Pieterse CMJ, Voesenek LACJ, et. al. Perception of low red : far-red ratio compromises both salicylic acid- and jasmonic acid-dependent pathogen defences in Arabidopsis. Plant J. 2013; 90–103. doi:10.1111/tpj.12203
- Marcela A´vila-Pe´rez, Hellingwerf KJ, Kort R. Blue Light Activates the σ^B-Dependent
 Stress Response of *Bacillus subtilis* via YtvA. J Bacteriol. 2006;188: 6411–6414.
 doi:10.1128/JB.00716-06
- 795 47. Purcell EB, Siegal-Gaskins D, Rawling DC, Fiebig A, Crosson S. A photosensory two 796 component system regulates bacterial cell attachment. Proc Natl Acad Sci. 2007;104:
 797 18241–18246. doi:10.1073/pnas.0705887104
- 798 48. Swartz TE, Tseng T, Frederickson MA, Paris G, Comerci DJ, Rajashekara G, et al. Blue Light–Activated Histidine Kinases: Two-Component Sensors in Bacteria. Science.
 2007;317: 1090–1094.
- 49. Curtis AM, Bellet MM, Sassone-corsi P, Neill LAJO. Review Circadian Clock Proteins and Immunity. Immunity. 2014;40: 178–186. doi:10.1016/j.immuni.2014.02.002
- Scheiermann C, Kunisaki Y, Frenette PS. Circadian control of the immune system. Nat Rev Immunol. 2013;13: 190–198. doi:10.1038/nri3386
- Donnell AJO, Schneider P, Mcwatters HG, Reece SE. Fitness costs of disrupting circadian rhythms in malaria parasites. 2011; 2429–2436. doi:10.1098/rspb.2010.2457
- Edgar RS, Stangherlin A, Nagy AD, Nicoll MP, Efstathiou S, O'Neill JS, et al. Cell autonomous regulation of herpes and influenza virus infection by the circadian clock. Proc Natl Acad Sci. 2016;113: 10085–10090. doi:10.1073/pnas.1601895113
- Sundar IK, Ahmad T, Yao H, Hwang J, Gerloff J, Lawrence BP, et al. Influenza A virusdependent remodeling of pulmonary clock function in a mouse model of COPD. Sci Rep. 2015;5: 1–14. doi:10.1038/srep09927
- 813 54. Rice LB. Federal Funding for the Study of Antimicrobial Resistance in Nosocomial Pathogens: No ESKAPE. 2008;197: 1079–1081. doi:10.1086/533452
- Tacconelli E, Carmell Y, Harbarth S, Kahlmeter G, Kluytmans J, Mendelson M, et al. Global priority list of antibiotic-resistant bacteria to guide research, discovery, and development of new antibiotics. WHO Press Release. 2017.
- Gibson DG, Young L, Chuang R-Y, Venter JC, Hutchison C a, Smith HO, et al. Enzymatic assembly of DNA molecules up to several hundred kilobases. Nat Methods. 2009;6: 343–5. doi:10.1038/nmeth.1318
- Hmelo LR, Borlee BR, Almblad H, Love ME, Randall TE, Tseng BS, et al. Precision-engineering the *Pseudomonas aeruginosa* genome with two-step allelic exchange. Nat Protoc. 2015;10: 1820–41. doi:10.1038/nprot.2015.115
- Winsor GL, Griffiths EJ, Lo R, Dhillon BK, Shay JA, Brinkman FSL. Enhanced annotations and features for comparing thousands of Pseudomonas genomes in the Pseudomonas genome database. Nucleic Acids Res. 2016;44: D646–D653. doi:10.1093/nar/gkv1227
- 828 59. Kumar S, Stecher G, Li M, Knyaz C, Tamura K. MEGA X: Molecular Evolutionary 829 Genetics Analysis across Computing Platforms. Mol. Biol. Evol. 2018; 35:1547–1549.

Figure 1

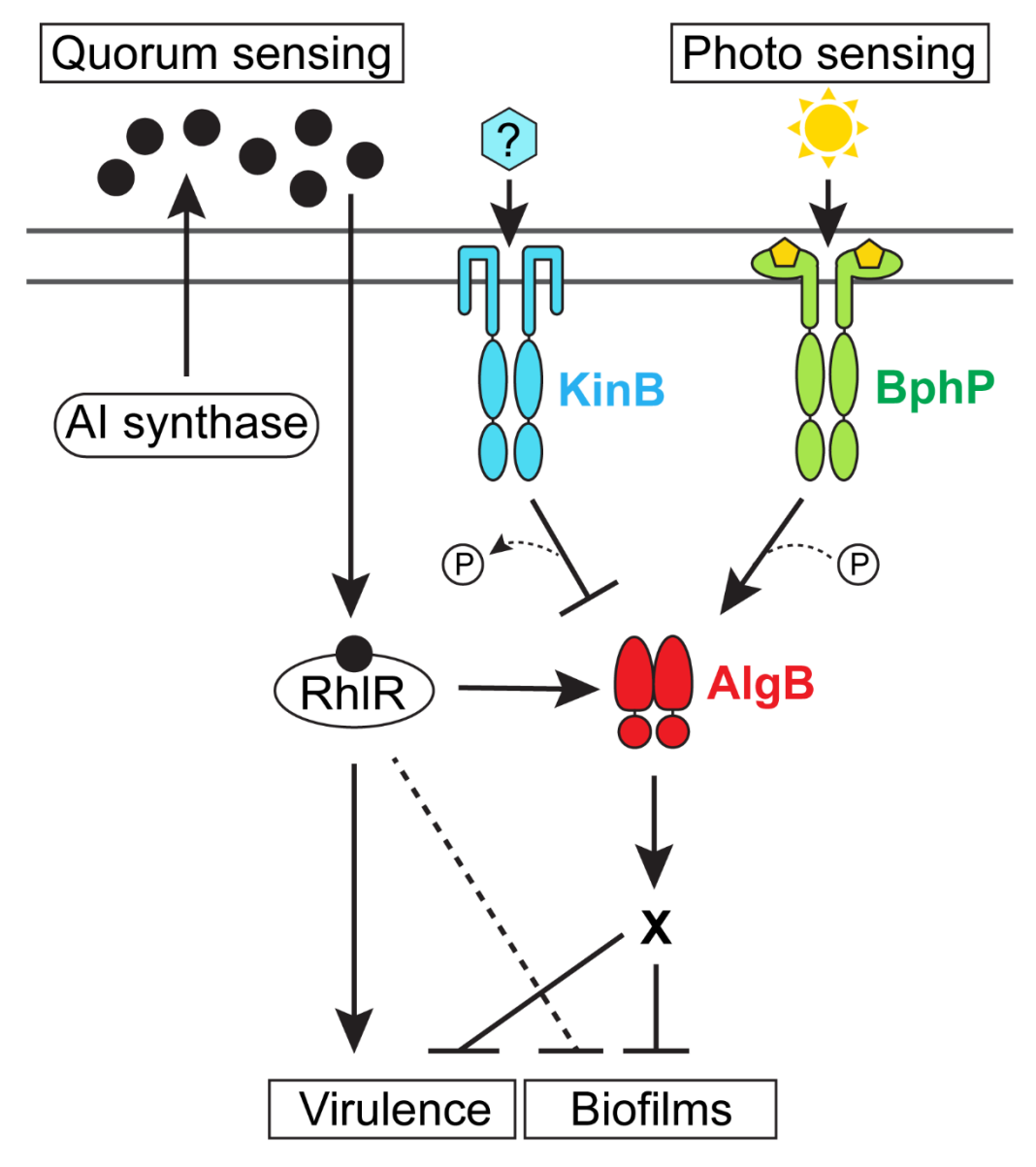


Fig 1. Model for *P. aeruginosa* integration of quorum-sensing and photo-sensing information into the control of virulence and biofilm development. The RhIR quorum-sensing receptor binds its cognate autoinducer (AI) produced by either the RhII or PqsE autoinducer synthase (black circles) at high cell density [22]. The RhIR-AI complex represses biofilm formation and virulence gene expression by activating transcription of the *algB-kinB* operon encoding the KinB HK and the AlgB RR, the latter a repressor of biofilm formation. KinB antagonizes AlgB by dephosphorylation. The stimulus (blue hexagon) for KinB is unknown. Photo sensing stimulates

the BphP HK to auto-phosphorylate, and subsequently transfer the phosphoryl group to AlgB to activate AlgB. AlgB~P activates transcription of genes required for repression of group behaviors such as biofilm formation and virulence. A "P" in a circle denotes addition or removal of a phosphate moiety. X denotes that the genes functioning downstream of AlgB in the process are not known. The RhIR-Al complex directly activates virulence gene expression and also represses biofilm formation by additional unknown mechanisms (dotted line).

Figure 2

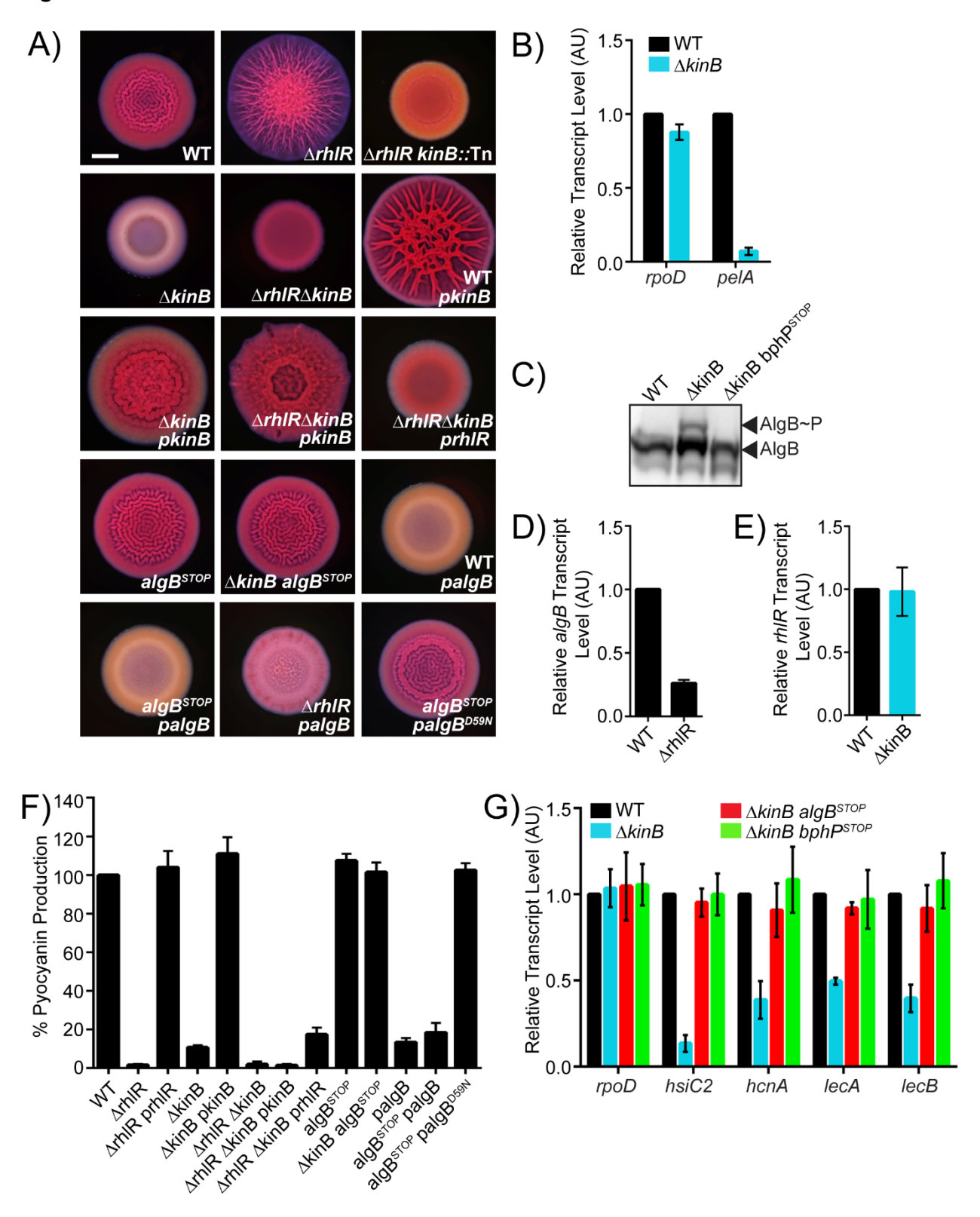


Fig 2. RhIR represses biofilm formation via KinB. A) Colony biofilm phenotypes of WT PA14 and the designated mutants on Congo red agar medium after 72 h of growth. kinB::Tn refers to a mutant identified in a genetic screen harboring a transposon insertion in kinB. pkinB. prhIR. and palgB refer to kinB, rhlR, and algB, respectively, under the Plac promoter on pUCP18. Scale bar for all images is 2 mm. B) Relative expression levels of rpoD and pelA measured by qRT-PCR in WT and $\Delta kinB$ mutant biofilms grown as in (A). C) Phos-tag Western blot analysis of the indicated strains probed for 3xFLAG-AlqB. D) Relative alqB transcript levels measured by qRT-PCR in WT PA14 and the $\triangle rhlR$ mutant grown planktonically to OD₆₀₀ = 1.0. E) Relative rhlR transcript levels measured by qRT-PCR in WT PA14 and the $\Delta kinB$ mutant grown planktonically to OD₆₀₀ = 1.0. F) Pyocyanin production (OD₆₉₅) was measured in WT PA14 and the designated mutants. Production from the WT was set to 100%. G) Relative expression of rpoD, hsiC2, hcnA, lecA, and lecB measured by qRT-PCR in WT PA14 and the designated mutants grown planktonically to OD₆₀₀ = 1.0. rpoD is used as the control for comparison. For panels B, D, E and G, data were normalized to 16S RNA levels and the WT levels were set to 1.0. AU denotes arbitrary units. For data in panels B, D, E, F, and G, error bars represent standard error of the mean (SEM) for three biological replicates.

Figure 3

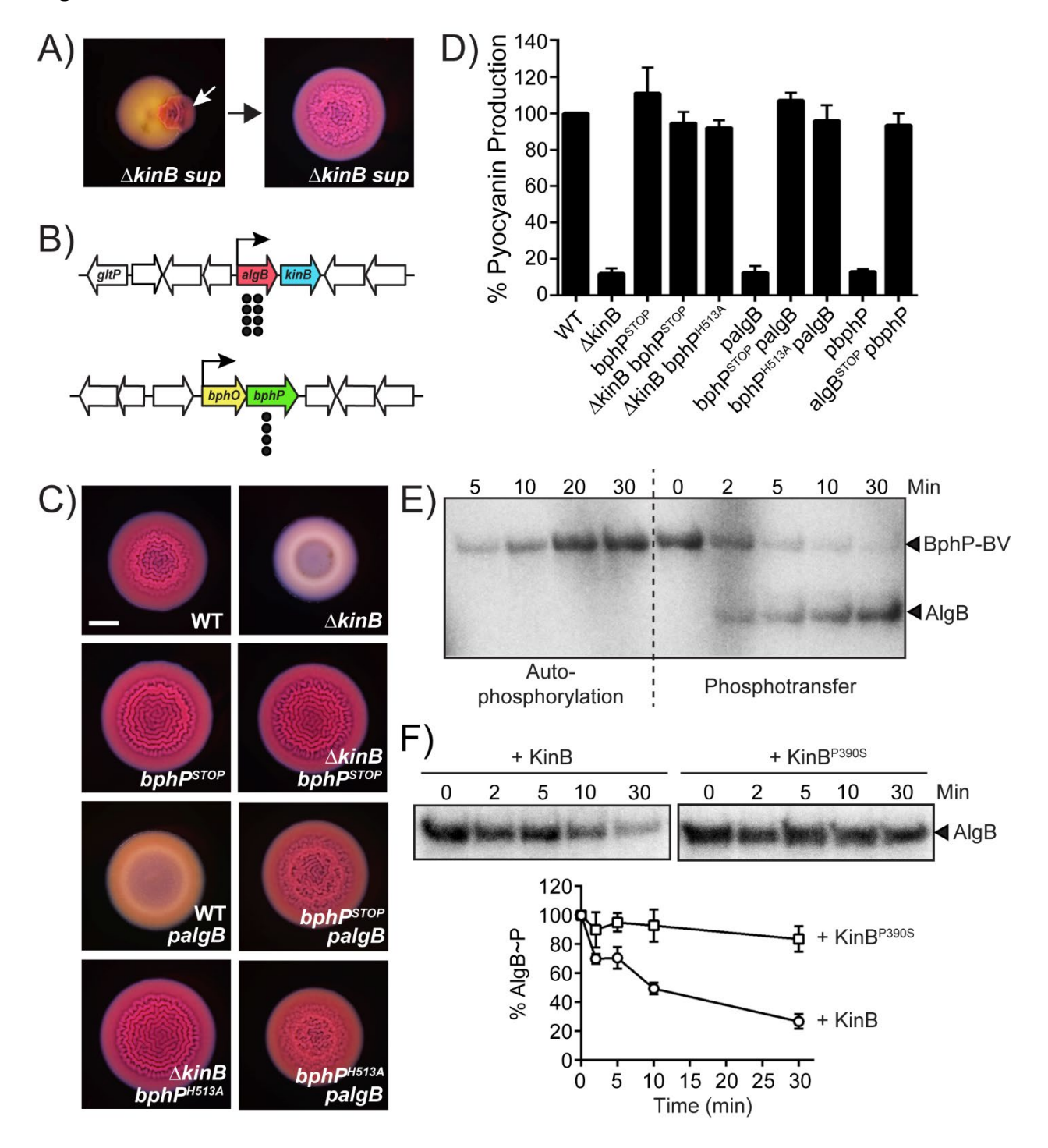


Fig 3. BphP is the cognate HK for AlgB. A) Shown is a representative isolation of a suppressor mutation of the $\Delta kinB$ smooth biofilm phenotype. The white arrow in the left panel indicates a region of rugose sectoring in the $\Delta kinB$ smooth biofilm that is diagnostic of the emergence of a

suppressor mutation. The right panel shows the biofilm phenotype of a mutant following isolation. B) Chromosomal arrangements of the algB (red), kinB (blue), bphO (yellow), and bphP (green) genes. Large white arrows represent open reading frames (lengths not to scale), black bent arrows indicate promoters, and black circles indicate the locations of suppressor mutations. C) Colony biofilm phenotypes of WT PA14 and the designated mutants on Congo red agar medium after 72 h of growth. palgB refers to algB under the Plac promoter on the pUCP18 plasmid. Scale bar is 2 mm for all images. D) Pyocyanin production (OD₆₉₅) was measured in WT PA14 and the designated mutants. *pbphP* refers to *bphP* under the P_{lac} promoter on the pBBR-MCS5 plasmid. Error bars represent SEM for three biological replicates. E) Autophosphorylation of BphP-BV and phosphotransfer to AlgB. (Left) Autophosphorylation of BphP-BV was carried out for 30 min and samples were removed at the indicated times for electrophoresis. (Right) An equimolar amount of AlgB was added to P~BphP-BV for 30 min and samples were removed at the indicated times for electrophoresis. F) Dephosphorylation of AlgB~P by KinB or KinB^{P390S}. Phosphotransfer to AlgB from P~BphP-BV was carried out for 30 min. ATP was removed from the reaction, and either KinB or KinB^{P390S} was added. Samples were removed at the indicated times for electrophoresis. The top panel shows representative images of gels. The bottom graph shows % AlgB~P levels at each time point with SEM for three independent replicates. Band intensities for AlgB~P when KinB was added (circles) and when KinB^{P390S} was added (squares) were normalized to the level at time zero level. To assess the quality of protein preparations used in panels E and F, see Fig. S4B.

Figure 4

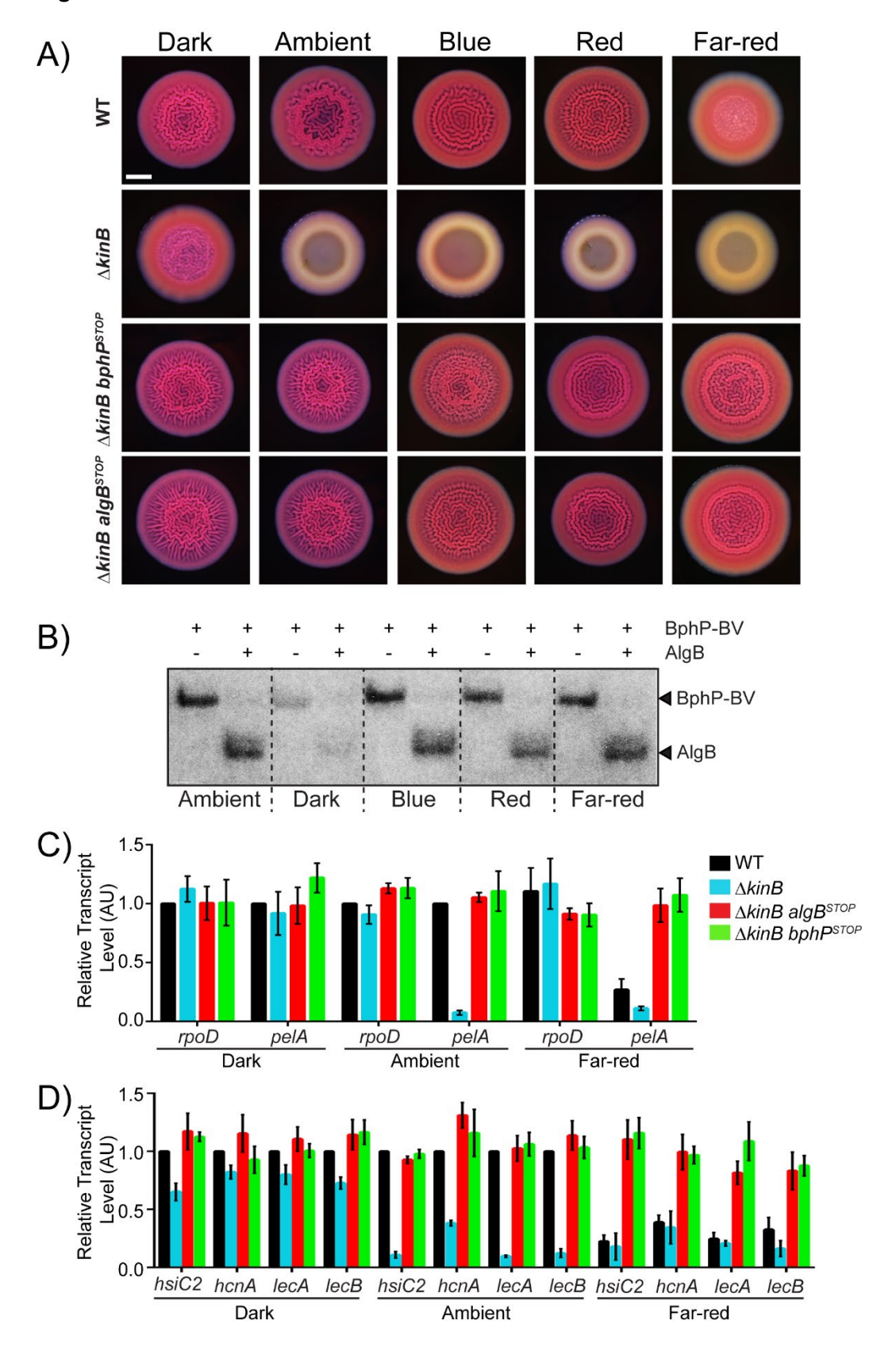


Fig 4. Photo sensing, via the BphP-AlgB phosphorelay, represses group behaviors in *P. aeruginosa*. A) Colony biofilm phenotypes are shown for WT PA14 and the designated mutants on Congo red agar medium after 72 h of growth under the indicated light conditions. Scale bar is 2 mm for all images. B) Autophosphorylation of the BphP-BV complex was carried out for 30 min (left lane in each pair) followed by addition of AlgB (right lane in each pair) for an additional 30 min under the indicated light conditions. C) Relative expression of *rpoD* and *pelA* as measured by qRT-PCR in WT PA14 and the designated mutant strains grown as biofilms as in (A) in darkness, ambient light, and far-red light. D) Relative expression of *hsiC2*, *hcnA*, *lecA*, and *lecB* measured by qRT-PCR in WT PA14 and the designated mutants grown as biofilms as in (A) and light conditions as in (B). For panels B and C, data were normalized to 16S RNA levels and the WT levels were set to 1.0. AU denotes arbitrary units and error bars represent SEM for three biological replicates.

Figure 5

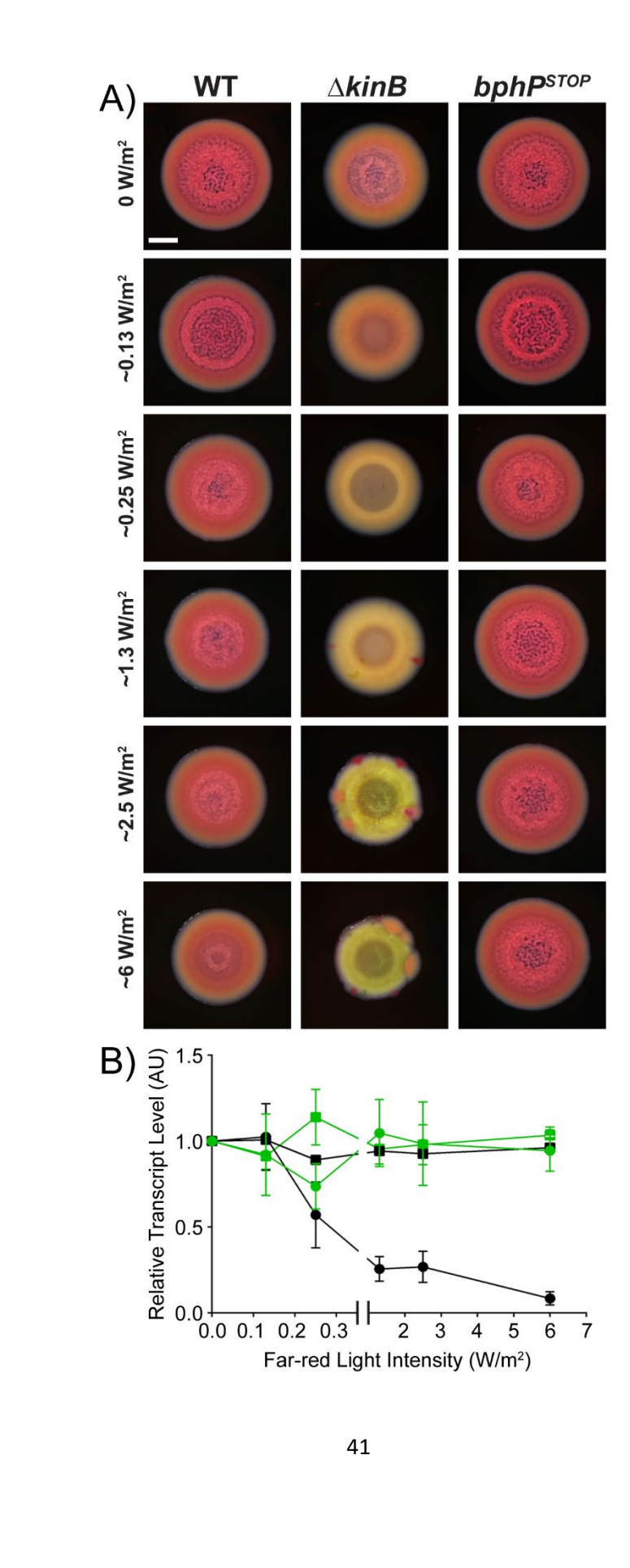


Fig 5. Far-red light intensity controls biofilm formation. A) Colony biofilm phenotypes are shown for WT PA14 and the designated mutants on Congo red agar medium after 72 h of growth under the indicated far-red light intensities. Scale bar is 2 mm for all images. B) Relative expression of *rpoD* (squares) and *pelA* (circles) measured by qRT-PCR in WT PA14 (black) and in the *bphP*^{STOP} mutant (green) grown as biofilms as in (A). Data were normalized to 16S RNA levels and the WT levels at 0 mW/m² far-red light were set to 1.0. AU denotes arbitrary units and error bars represent SEM for three biological replicates.

Figure 6

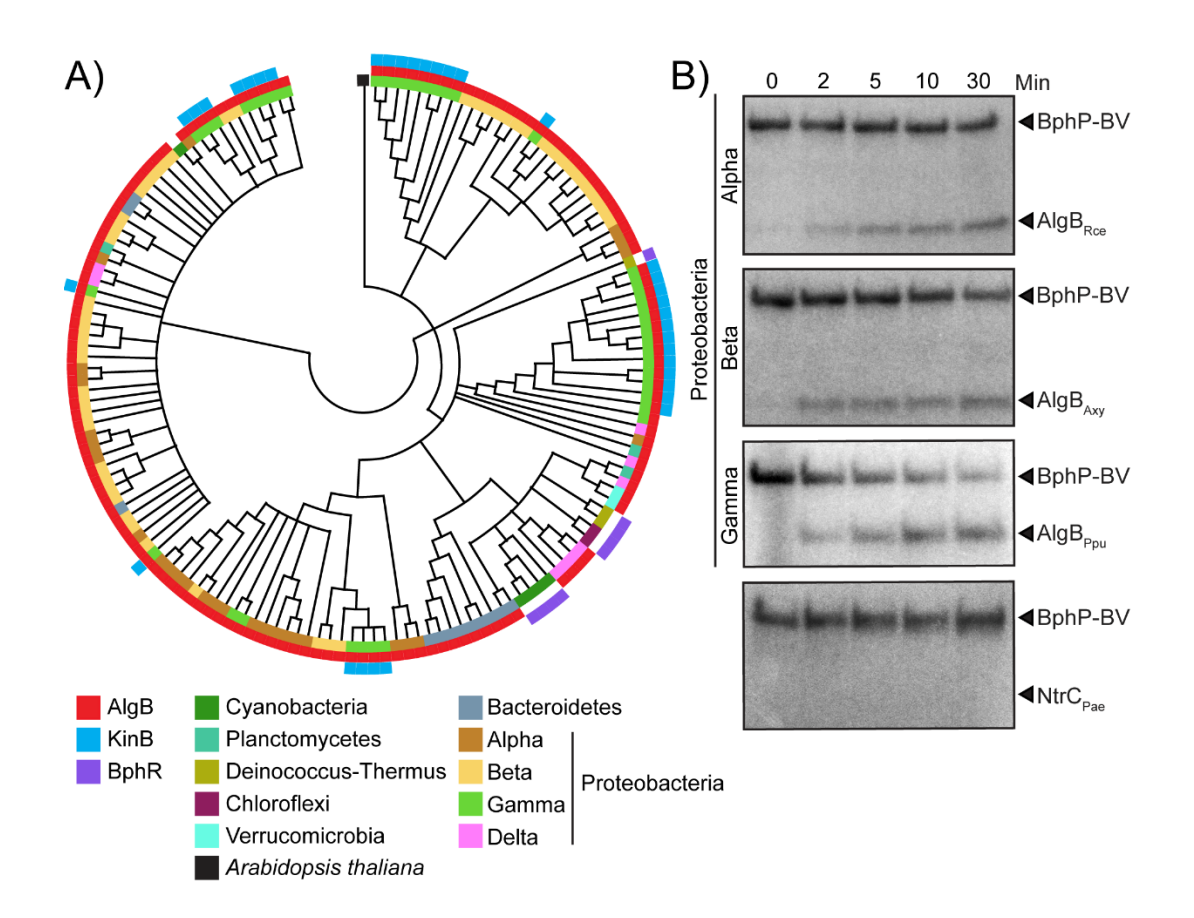
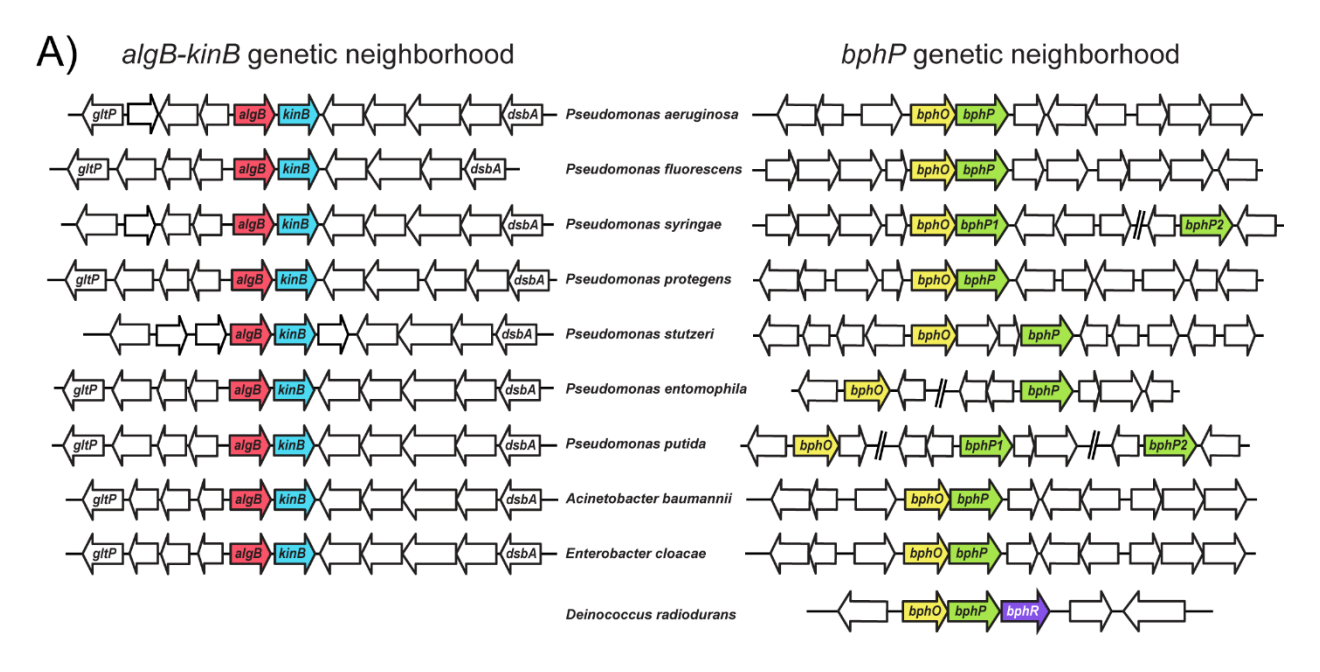
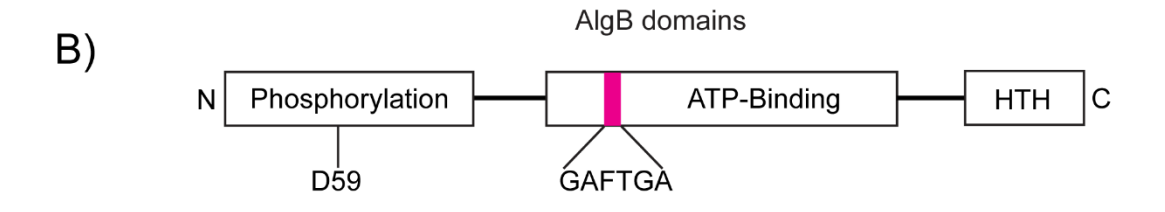
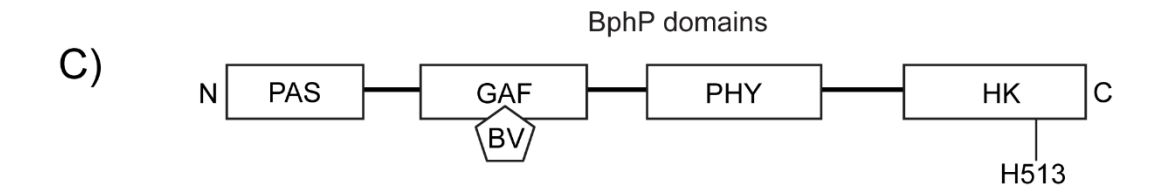


Fig 6. The BphP-AlgB phosphotransfer relay is conserved in diverse bacteria. A) Maximum likelihood-based phylogenetic tree for BphP showing the 150 closest orthologs to *P. aeruginosa* BphP, generated using MEGA-X software [59]. Co-occurrences of AlgB and KinB are depicted in red and blue, respectively. BphR is shown in purple. The other colors indicate bacterial phyla. The black square indicates *Arabidopsis thaliana* as the root of the tree. B) *In vitro* phosphorylation of AlgB orthologs from the α-Proteobacterium *Rhodospirillum centenum* (Rce), the β-Proteobacterium *Achromobacter xylosoxidans* (Axy), and the γ-Proteobacterium *Pseudomonas putida* (Ppu) by *P. aeruginosa* BphP-BV that had been autophosphorylated for 30 min. The bottom panel shows that phospho-transfer from *P. aeruginosa* P~BphP-BV to *P. aeruginosa* NtrC does not occur. To assess the quality of the protein preparations used in panel B, see Fig S4B.

S1 Figure



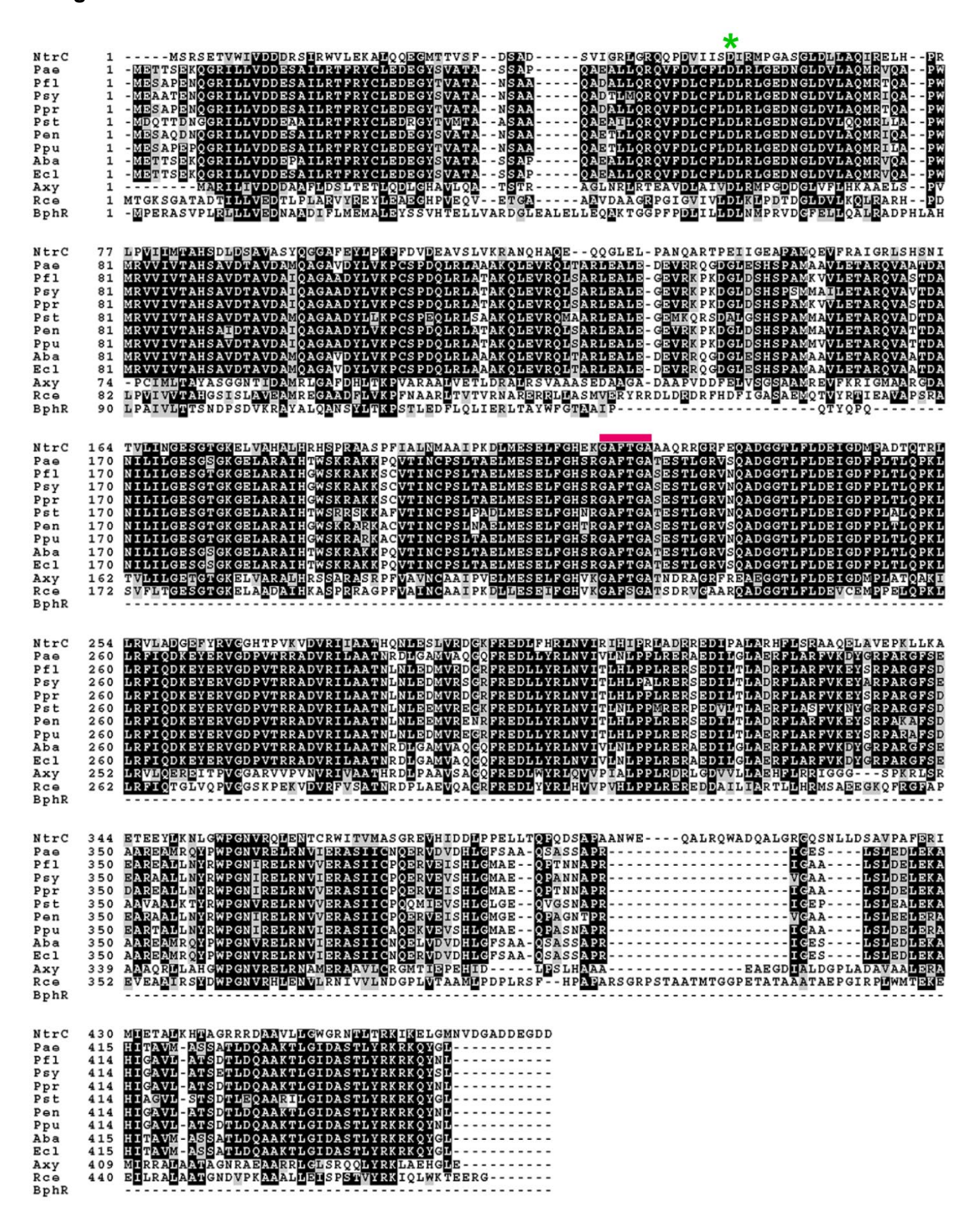




S1 Fig. Gene conservation for KinB, AlgB, BphO, and BphP, and domain architectures of the AlgB and BphP proteins. A) The genes flanking *kinB*, *algB*, *bphO*, and *bphP* are diagrammed for the indicated genomes. The relative gene positions and orientations are accurate, but gene lengths are not to scale. B) The domain architecture of the AlgB monomer is shown. Residue 59 is required for phosphorylation, the GAFTA motif, indicated by the magenta shading, is required for interaction with σ^{54} , and HTH refers to the helix-turn-helix DNA binding domain.

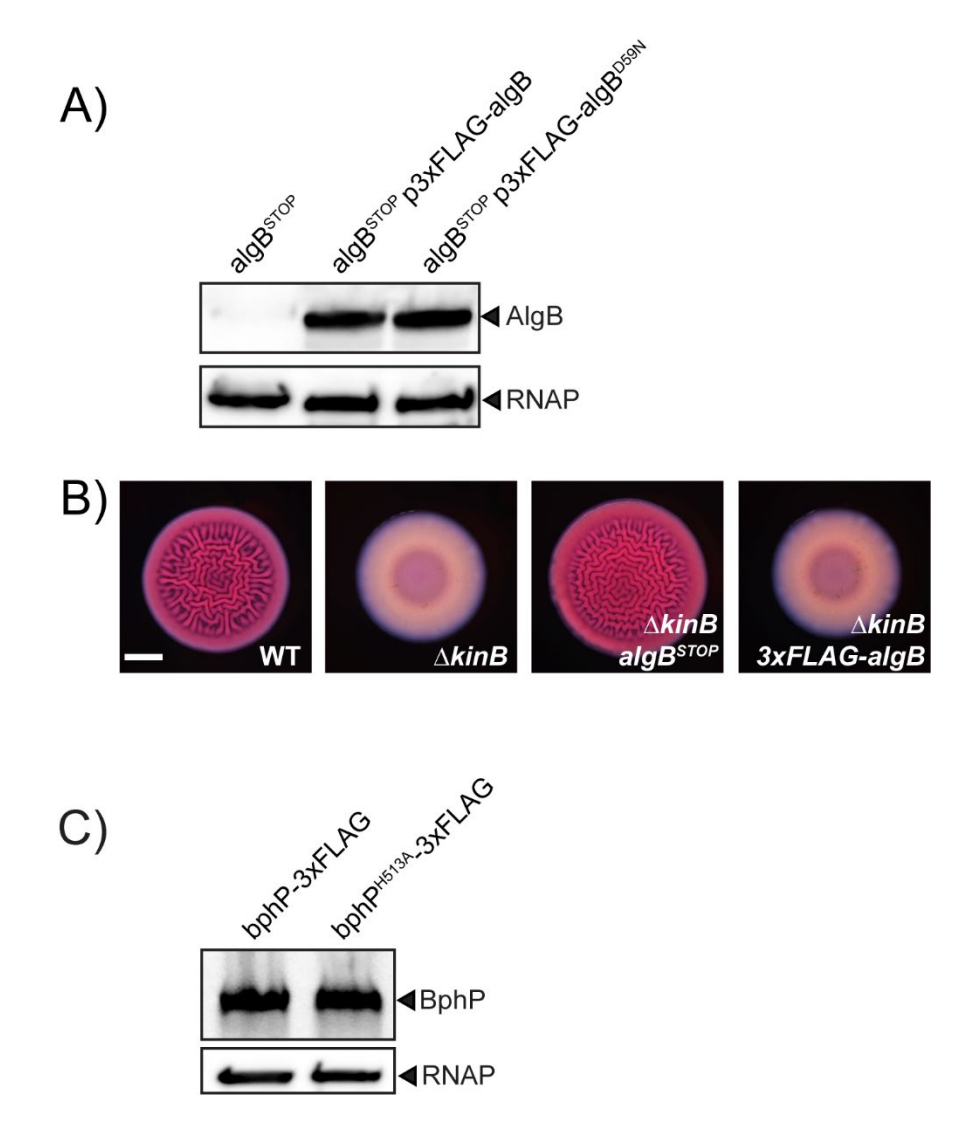
Adapted from [28]. C) Domain organization of the BphP monomer consisting of the PAS, GAF, PHY, and HK domains is shown. Biliverdin (BV) binds to the GAF domain and residue H513 is required for autophosphorylation. Adapted from [15].

S2 Figure



S2 Fig. Multiple sequence alignment for AlgB orthologs. Primary sequence alignment of NtrC (first line) and AlgB (second line) from P. aeruginosa (Pae), and AlgB orthologs (third through twelfth lines) from Pseudomonas fluorescens (Pfl), Pseudomonas syringae (Psy), Pseudomonas Pprotegens (Ppr), Pseudomonas Pseudomonas

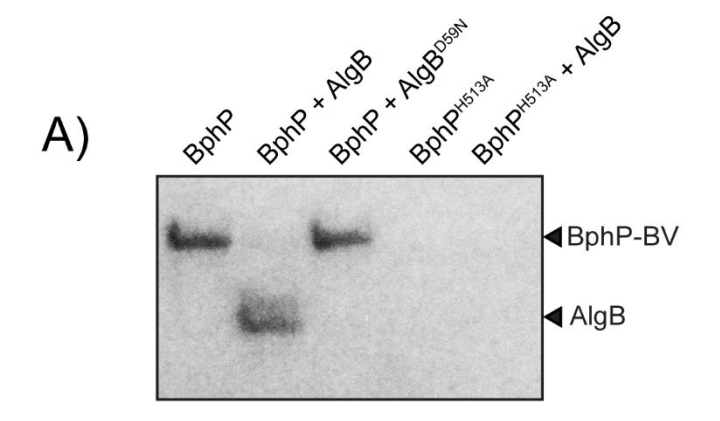
S3 Figure

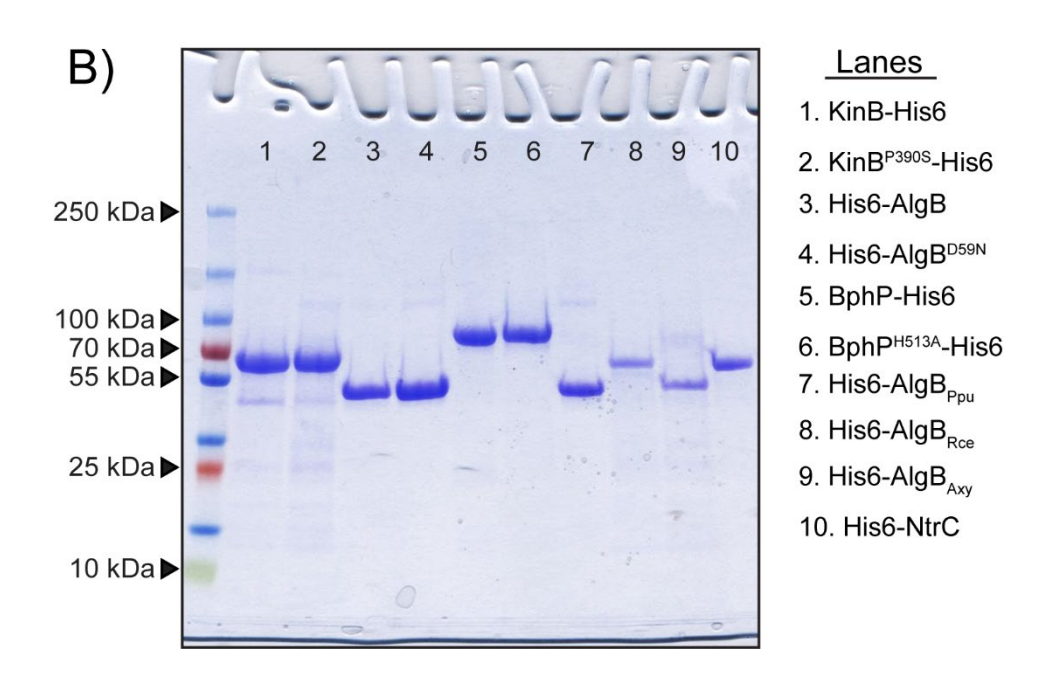


S3 Fig. AlgB^{D59N}, KinB^{P390S} and BphP^{H513A} are produced and stable in *P. aeruginosa*. A) Western blot analysis of whole cell lysates from the indicated strains, all of which have the $algB^{STOP}$ allele at the native locus in the genome and carry an empty vector or 3xFLAG-algB or 3xFLAG- $algB^{D59N}$ on the pBBR1-MCS5 plasmid under the P_{lac} promoter. The same cell lysates were probed for RNAP as the loading control. B) Colony biofilm phenotypes of WT PA14, and the $\Delta kinB$, $\Delta kinB$ $algB^{STOP}$, and $\Delta kinB$ 3xFLAG-algB mutants. Scale bar is 2 mm. C) SDS-PAGE analysis of whole cell lysates from the indicated strains. The gel was stained for SNAP using SNAP-Cell® 647-SiR fluorescent substrate (NEB). Lysozyme was added as the loading control.

D) Colony biofilm phenotypes of the WT, *kinB-SNAP*, and *kinB^{P390S}-SNAP* strains. Scale bar is 2 mm. E) Western blot analysis of whole cell lysates from the indicated strains. The same cell lysates were probed for RNAP as the loading control.

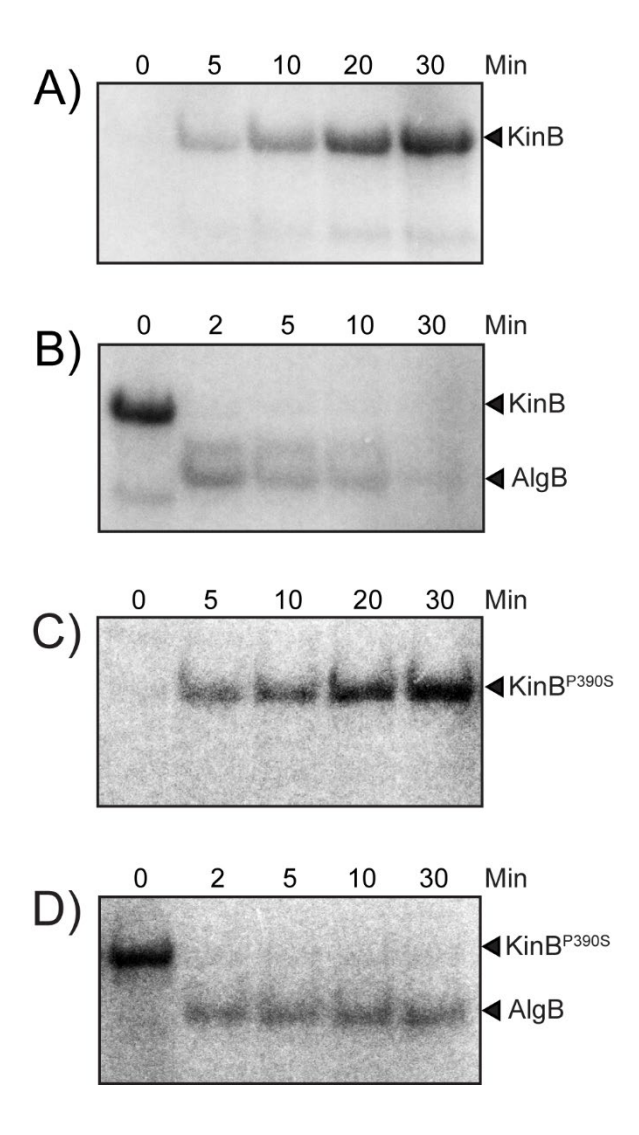
S4 Figure





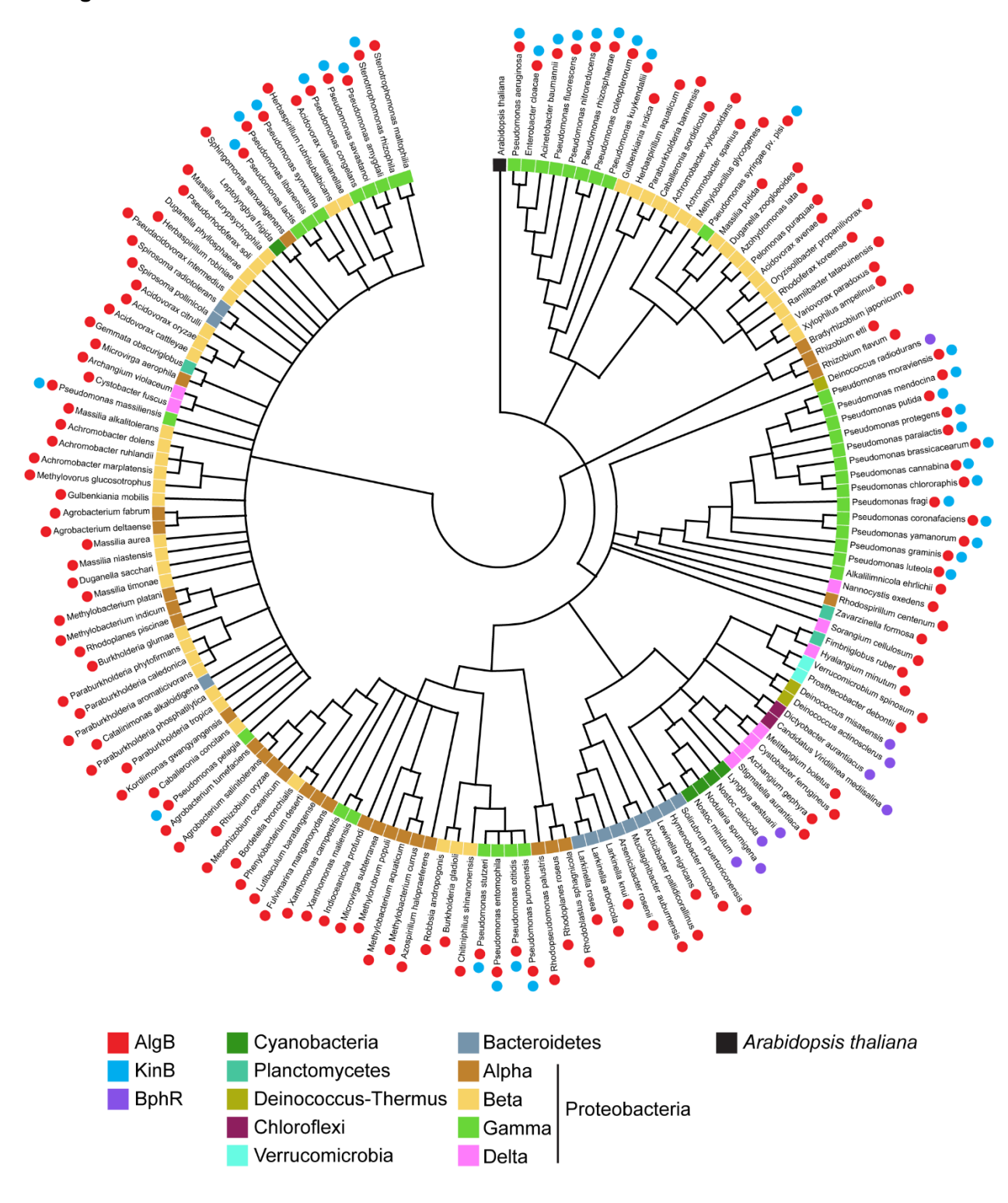
S4 Fig. Phosphotransfer from BphP to AlgB *in vitro*. A) Autophosphorylation of the BphP-BV complex was carried out for 30 min (left most lane) followed by addition of AlgB (second lane) or AlgB^{D59N} (third lane) for an additional 30 min. The kinase-defective BphP^{H513A}-BV complex was incubated with radiolabeled ATP for 30 min (fourth lane), followed by addition of AlgB (fifth lane) for an additional 30 min. B) SDS-PAGE gel stained with Commassie Brilliant Blue showing the indicated purified proteins. 10 μ L of a 20 μ M stock of each protein was loaded.

S5 Figure



S5 Fig. KinB and KinB^{P390S} **can phosphorylate AlgB** *in vitro*. A) Autophosphorylation of KinB was carried out for 30 min and samples were removed at the indicated times. B) An equimolar amount of AlgB was added to KinB that had been autophosphorylated for 30 min as in (B). Samples were taken at the indicated times. C and D) As in A and B, respectively, but for the phosphatase-deficient protein KinB^{P390S}.

S6 Figure



S6 Fig. The BphP-AlgB module is conserved in diverse bacteria. Enlarged maximum likelihood-based phylogenetic tree for BphP from Fig 6A showing the 150 closest orthologs to *P. aeruginosa* BphP. Co-occurrences of AlgB and KinB are depicted using red and blue dots, respectively. The presence of BphR is shown by purple dots. The colored squares indicate the corresponding bacterial phyla. The black square indicates *Arabidopsis thaliana* as the root of the tree.

TABLE S1: Transposon insertion locations

Gene name and description of encoded protien
dcd, deoxycytidine triphosphate deaminase
hypothetical protein
zbdP, zinc-binding dehydrogenase
wbpM, nucleotide sugar epimerase/dehydratase
pelA, extracellular polysaccharide biosynthesis protein
pelB, extracellular polysaccharide biosynthesis protein
dsbG, disulfide isomerase/thiol-disulfide oxidase
pvdG, pyoverdine synthetase
pvdF, pyoverdine synthetase
hypothetical protein
hmgA, homogentisate 1,2-dioxygenase
hypothetical protein
gltA, type II citrate synthase
hypothetical protein
pilC, type 4 fimbrial biogenesis protein
hypothetical protein
pvrS, two-component sensor kinase
pilQ, type 4 fimbrial biogenesis protein
pilM, type 4 fimbrial biogenesis protein
kinB, two-component sensor kinase

a: annotation from www.pseudomonas.com [58]

TABLE S2: Suppressor mutations of the $\Delta kinB$ smooth biofilm phenotype

Suppressor	PA14 ID ^a	Gene name	Nucleotide position	Mutation
SM1045	PA14_72380	algB	6447033	∆10 bp
SM1062	PA14_72380	algB	6447033	∆10 bp
SM1063	PA14_72380	algB	6447033	∆10 bp
SM1064	PA14_72380	algB	6447033	∆10 bp
SM1067	PA14_10700	bphP	919652	∆1603 bp
SM1068	PA14_72380	algB	6447064	∆1 bp
SM1072	PA14_72380	algB	6447033	∆10 bp
SM1073	PA14_72380	algB	6447033	∆10 bp
SM1074	PA14_10700	bphP	921631	G → T
SM1149	PA14_72380	algB	6446399	∆21 bp
SM1150	PA14_10700	bphP	921151	∆12 bp
SM1151	PA14_10700	bphP	921731	G → T

a: annotation from www.pseudomonas.com [58]

TABLE S3: Bacterial strains

Strain	Description	Reference
UCBPP-PA14	Wild type Pseudomonas aeruginosa	Laboratory stock
SM32	ΔrhIR	[21]
SM1040	∆rhIR ∆kinB	This study
SM1050	∆kinB	This study
SM1111	pUCP18- <i>P_{lac}-kinB</i>	This study
SM1112	∆rhIR ∆kinB pUCP18-P _{lac} -kinB	This study
SM1116	Δ kinB pUCP18- P_{lac} -kinB algB STOP	This study
SM1204	algB ^{STOP}	This study
SM1212	∆kinB algB ^{STOP}	This study
SM1278	∆kinB bphP ^{STOP}	This study
SM1282	bphP ^{STOP}	This study
SM1286	pUCP18-P _{lac} -algB	This study
SM1303	∆rhIR pUCP18-P _{lac} -algB	This study
SM1326	<i>bphP^{STOP}</i> pUCP18- <i>P_{lac}-algB</i>	This study
SM1377	3xFLAG-algB	This study
SM1378	∆kinB 3xFLAG-algB	This study
SM1386	∆kinB bphP ^{H513A}	This study
SM1387	algB ^{STOP} pUCP18-P _{lac} -algB	This study
SM1388	bphPH513A pUCP18-Plac-algB	This study
SM1413	algB ^{STOP} pBBR1-MCS5-P _{lac} -3xFLAG-algB	This study
SM1514	3xFLAG-algB kinB-SNAP	This study
SM1523	3xFLAG-algB kinB ^{P390S} -SNAP	This study
SM1535	pBBR-MCS5-P _{lac} -bphP	This study
SM1543	algB ^{STOP} pBBR1-MCS5-P _{lac} -bphP	This study
SM1562	algB ^{STOP} pBBR1-MCS5-P _{lac} -3xFLAG-algB ^{D59N}	This study
SM1563	algB ^{STOP} pUCP18-P _{lac} -algB ^{D59N}	This study
SM1617	bphP-3xFLAG	This study
SM1618	bphP ^{H513A} -3xFLAG	This study

TABLE S4: Plasmids

Plasmid	Description	Reference
pEXG2	Allelic exchange vector with pBR origin, gentamicin resistance, <i>sacB</i>	(Hmelo et al., 2015)
pUCP18	E. coli-Pseudomonas Amp ^r shuttle vector	Laboratory stock
pBBR1-MCS5	E. coli-Pseudomonas Gent ^r shuttle vector	Laboratory stock
plT2	ISlacZ/hah transposon mutagenesis vector	(Jacobs et al., 2003)
pET21b	Protein expression vector, Amp ^r	Laboratory stock
pET28b	Protein expression vector, Kan ^r	Laboratory stock
pSP201	pET21b-bphP-His6	This study
pSP202	pET21b-kinB-His6	This study
pSP203	pET28b-His6-algB	This study
pSP204	pET21b-bphP ^{H513A} -His6	This study
pSP205	pET28b-His6-algBPpu	This study
pSP206	pET28b-His6-algB ^{D59N}	This study
pSP207	pET21b-kinB ^{P390S} -His6	This study
pSP208	pET28b-His6-ntrC	This study
pSP209	pET28b-His6-algBRce	This study
pSP210	pET28b-His6-algBAxy	This study